Function of the urethral tuft cell deciphered by genetic models allowing cell type-specific activation

Inaugural Dissertation

submitted to the

Faculty of Medicine

in partial fulfillment of the requirements

for the PhD-Degree

of the Faculties of Veterinary Medicine and Medicine

of the Justus Liebig University Giessen

by

Lafee, Mahmoud

from

Amman/Jordan

Giessen 2025

From the Institute of Anatomy and Cell Biology

Director/Chairman: Prof. Dr. Ralf Middendorff

of the Faculty of Medicine of the Justus Liebig University Giessen

First Reviewer and Committee Member: Prof. Dr. Wolfgang Kummer

Second Reviewer and Committee Member: Prof. Dr. Stefanie Kürten

Vice-chair and Committee Member: Prof. Dr. Christoph Rummel

Chairman and Committee Member: Prof. Dr. Norbert Weissmann

Date of Doctoral Defense 04.02.2026

Table of content

Table of content

List of abbreviations

5-HT_2A	Serotonin 2 receptor family, subtype 2A
5-HT_2C	Serotonin 2 receptor family, subtype 2C
ACh	Acetylcholine
Adrenergic (α_1, α_2)	Alpha-1 and 2 adrenergic receptors
ATP	Adenosine triphosphate
BAC	Bacterial artificial chromosome
Ca^{2+}	Calcium ion
CFU	Colony-forming units
CGRP	Calcitonin gene-related peptide
ChAT	Choline acetyltransferase
ChR2	Channelrhodopsin-2
CLR	Calcitonin-like receptor
CNO	Clozapine N-oxide
CTL4	Choline transporter-like protein 4
D_2	Dopamine receptor 2
D_4	Dopamine receptor 4
DAG	Diacylglycerol
DAPI	4′,6-Diamidino-2-phenylindole
DCLK1	Doublecortin-like kinase 1
DMEM	Dulbecco’s modified eagles’s medium
DMSO	Dimethylsulfoxide
DREADD	Designer receptor exclusively activated by designer drugs
DRG	Dorsal root ganglia
eGFP	Enhanced green fluorescent protein
EMG	Electromyography
ENaC	Epithelial sodium channel
EtOH	Ethanol
EYFP	Enhanced yellow fluorescent protein
Gαgus	Gustducin
Gβγ	G beta-gamma complex
H^+	Hydrogen ion

List of abbreviations

H^+-ATPase	Hydrogen-ion adenosine triphosphatase
H1R	Histamine H1 receptor
HIV	Human immunodeficiency viruses
IL-13	Interleukin-13
IL-25	Interleukin-25
ILC2s	Innate lymphoid cells type 2
IQR	Interquartile range
IP_3	Inositol 1,4,5-triphosphate
K^+	Potassium ion
kDa	Kilodaltons
KO	Knockout
LPS	Lipopolysaccharides
LUT	Lower urinary tract
mAChRs	Muscarinic acetylcholine receptors
M_1–M_5	Muscarinic acetylcholine receptor subtypes 1-5
Na^+	Sodium ion
nAChRs	Nicotinic acetylcholine receptors
nAChRα3	Nicotinic acetylcholine receptor subunit α3
NK1R, NK2R, NK3R	Neurokinin receptors
OCT1-3	Organic cation transporters 1-3
OCTN1	Organic cation transporter novel member 1
PBS	Phosphate-buffered saline
pChAT	Peripheral type of ChAT
PFA	Paraformaldehyde
PLCβ2	Phospholipase C isoform β2
Pou2f3	POU Class 2 Homeobox 3
RAMP1	Receptor activity-modifying protein 1
RCP	Receptor component protein
SP	Substance P
TAS2R4	Taste receptor type 2 member 4
TAS2R10	Taste receptor type 2 member 10

List of abbreviations

TRPA1	Transient receptor potential cation channel subfamily A member 1
TRPM5	Transient receptor potential cation channel subfamily M member 5
TRPV1	Transient receptor potential cation channel subfamily V member 1
UCCC	Urethral cholinergic chemosensory cells
UPEC	Uropathogenic *Escherichia coli*
UTC	Urethral tuft cell
UTIs	Urinary tract infections
VAChT	Vesicular acetylcholine transporter

Introduction

1. Introduction

The urethra constitutes the terminal segment of the urinary tract and functions as the channel for the excretion of urine from the bladder. At this stage, urine undergoes no further modification, which is why the urethra is sometimes regarded as a less significant component of the urinary system. Nevertheless, it represents a critical potential portal of entry for ascending infections, including urinary tract infections (UTIs), human immunodeficiency viruses (HIV), and certain parasitic infestations.

1.1 Structure of the mouse urethra

1.1.1 Male urethra

In male mice, the urethra extends from the trigone of the urinary bladder to the external urethral orifice and is divided into two main regions: the membranous urethra and the penile urethra. The membranous urethra is relatively narrow and is positioned in close association with the prostate, seminal vesicles, coagulating glands, and vas deferens. This segment maintains a typical structural and functional organization comparable to other mammals. The penile urethra traverses the penis and terminates at the glans. Its lumen is lined by transitional epithelium (urothelium), while the distal external urethral orifice is covered by stratified squamous epithelium. The underlying lamina propria consists of loose connective tissue. Within this region, the periurethral glands (glands of Littré) are found. These are small, mucus-secreting glands that open into the penile urethra. Secretions from the seminal vesicles, coagulating glands (anterior prostate), and bulbourethral glands combine within the urethra to form a coagulum, also known as the copulatory plug, which is commonly observed in mice after mating (Treuting et al., 2017).

1.1.2 Female urethra

The female urethra measures approximately 9 mm in length and can be distinguished histologically into several layers. The urethral lumen is bordered by the tunica mucosa, whose epithelial lining varies along its course.

- **Proximal region (near the bladder):** lined with urothelium.
- **Middle region:** composed of multilayered cuboidal epithelium with up to eight cell layers.

- **Distal region:** transitions first to multilayered non-keratinized squamous epithelium and, near the external urethral opening (ostium urethrae externum), to multilayered keratinized squamous epithelium.

Beneath the epithelium lies the lamina propria, composed primarily of collagen fibers and fibroblasts, traversed by numerous myelinated and unmyelinated nerve fibers. In the distal half of the urethra, urethral glands are present. A venous plexus also permeates the loose connective tissue.

The muscular layer surrounding the urethra is predominantly circular and consists of both smooth and striated fibers. The ventral aspect is mainly occupied by striated muscle. The female urethra is separated from the adjacent vagina by a thin layer of loose connective tissue (Phillips and Davies 1980).

1.2 Urinary tract infections

Urinary tract infections (UTIs) are inflammatory conditions of the urinary tract caused by bacterial invasion, and they are typically characterized by pyuria and bacteriuria. The majority of UTIs result from ascending infections, where bacteria colonizing the urethra or periurethral space migrate into the bladder. Less commonly, hematogenous spread may occur, in which bacteria circulating in the bloodstream disseminate to the kidneys or bladder (Al Lawati et al., 2024) (Figure 1.1).

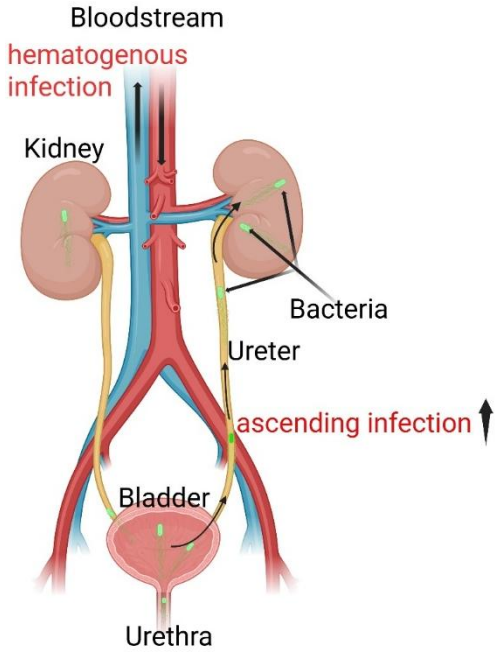

Figure 1.1: Schematic representation of the urinary tract system and possible routes of infection. Created with BioRender.

Introduction

UTIs are traditionally classified according to the site of infection. Lower tract infections include urethritis and cystitis, while upper tract infections comprise pyelonephritis, urosepsis, and infections of the male accessory sex glands. Additionally, UTIs are subdivided into uncomplicated and complicated categories (Mancuso et al., 2023).

- Uncomplicated UTIs occur in otherwise healthy individuals without predisposing risk factors.
- Complicated UTIs arise in patients with anatomical or functional abnormalities of the urinary tract, including obstruction, urinary retention, underlying comorbidities, pregnancy, immunodeficiency, or the presence of long-term catheters (Nielubowicz and Mobley 2010).

This classification is clinically important, as it guides both treatment strategies and prognosis.

1.2.1 Epidemiology

UTIs are among the most frequent bacterial infections worldwide (Measley, JR and Levison et al., 1991; Stamm and Norrby 2001). Routine data collected in 2013 by the Barmer GEK health insurance company in Germany highlight their prevalence: among insured women aged 12 years and older, 356,774 were diagnosed with a UTI, including 84,139 with acute cystitis and 7,969 with acute pyelonephritis. The overall prevalence in this population was 7.32%, with cystitis representing 1.73% and pyelonephritis 0.16%. Acute cystitis was particularly common in women aged 20–29 years and in those over 70 years (Gläske and Schicktanz 2016).

Epidemiological studies estimate that approximately 40% of women and 12% of men will experience at least one UTI in their lifetime. Among women, 27–48% develop recurrent infections (Foxman 2003).

In hospital environments, UTIs are a major source of morbidity, accounting for around 40% of all nosocomial infections. Furthermore, infections originating in the urinary tract contribute to 9–31% of septicemia cases, a complication associated with high mortality rates (Levy et al., 2012). Catheterization plays a central role in hospital-acquired infections: 70–80% are linked to indwelling catheters (Nicolle 2014). A European Centre for Disease Prevention and Control (ECDC) survey across 66 hospitals in

Europe found that 17.5% of inpatients had a transurethral indwelling catheter, making it the most frequently placed indwelling medical device (Zarb et al., 2012).

The economic burden of UTIs is considerable. In the United States alone, healthcare costs attributable to UTIs were estimated at 2.6 billion USD in 2006 (Nielubowicz and Mobley 2010).

Taken together, the high prevalence, recurrence rates, risk of severe complications, and significant healthcare costs underscore the global impact of UTIs. These factors also emphasize the importance of using experimental infection models, such as mice, to better understand host-pathogen interactions and to develop novel strategies for treatment and prevention.

1.2.2 Spectrum of pathogens

UTIs can be caused by a wide range of microorganisms, including both Gram-negative and Gram-positive bacteria, and in rare cases by fungi. However, among the bacterial pathogens, *Escherichia coli* plays the predominant role as the causative agent. Approximately 75% of all uncomplicated UTIs and 65% of complicated UTIs are attributed to colonization by uropathogenic *E. coli* (UPEC).

Other pathogens associated with uncomplicated UTIs, listed in descending order of frequency, include *Klebsiella pneumoniae, Staphylococcus saprophyticus, Enterococcus faecalis, Streptococcus agalactiae, Proteus mirabilis, Pseudomonas aeruginosa, Staphylococcus aureus,* and *Candida spp*. In complicated UTIs, UPEC remains the most common pathogen, but additional organisms are frequently involved. These include *Enterococcus spp., Klebsiella pneumoniae, Candida spp., Staphylococcus aureus, Proteus mirabilis, Pseudomonas aeruginosa,* and *Streptococcus agalactiae* (Ronald 2003; Flores-Mireles et al., 2015) (Figure 1.2).

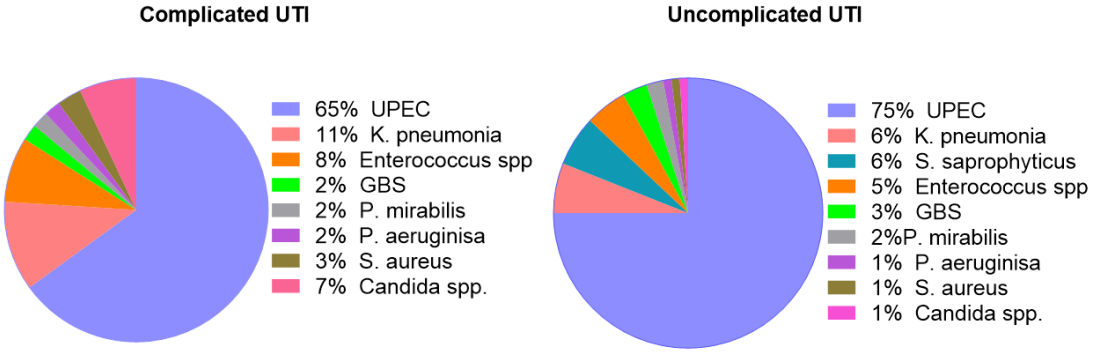

Figure 1.2: Spectrum of pathogens in uncomplicated and complicated UTIs. This figure modified from (Flores-Mireles et al., 2015).

UPEC strains differ from non-pathogenic commensal *E. coli* by possessing a variety of virulence factors that allow them to overcome host defenses and colonize the urinary tract. These include:

- **Surface structural components**, such as lipopolysaccharides (LPS), a polysaccharide capsule, flagella, pili, curli (thin aggregative fimbriae), non-fimbrial adhesins, and outer membrane proteins.
- **Secreted molecules**, including outer membrane vesicles and a range of toxins.
- **Specialized secretion systems** that facilitate delivery of effector molecules.
- **Iron acquisition mechanisms**, such as TonB-dependent uptake receptors and siderophore receptors, which enable survival in the iron-limited urinary tract environment (Terlizzi et al., 2017).

1.2.3 Risk factors

Risk factors for UTIs can be grouped into three categories: (1) factors increasing exposure to uropathogens, (2) factors facilitating bacterial colonization, and (3) factors enhancing the host response to colonization, thereby promoting symptom development.

For uncomplicated UTIs, key risk factors include female sex, prior UTIs, sexual activity, diabetes, obesity, use of spermicides, vaginal infections, trauma to the vaginal area, and genetic predisposition (Foxman 2014). The higher incidence in women is largely explained by anatomical differences: the female urethra averages only 3.1 cm, compared with 22.3 cm in men (Kohler et al., 2008; Pomian et al., 2018). Its shorter length, along with the close proximity of the urethral opening to the rectum, facilitates bacterial colonization by gastrointestinal pathogens (Brown and Foxman 2000; Kirjavainen et al., 2009).

For complicated UTIs, risk factors include urinary tract obstruction, urinary retention, long-term catheterization, pregnancy, and immunosuppression, all of which predispose patients to recurrent or severe infections (Nielubowicz and Mobley 2010).

1.2.4 Clinical symptoms, diagnostics and therapy

The clinical presentation of uncomplicated UTIs varies depending on the site of infection. In cases of cystitis, typical symptoms include dysuria (painful urination), urinary urgency, pollakiuria (increased urinary frequency), and suprapubic pain. When the infection progresses to pyelonephritis, additional manifestations such as flank pain, tenderness in the kidney region, and fever exceeding 38 °C are commonly observed (Kranz et al., 2017).

In rare instances, UTIs may be asymptomatic. It is important to distinguish these cases from asymptomatic bacteriuria, which is defined by the presence of $\geq 10^5$ colony-forming units (CFU) per milliliter of urine in the absence of clinical symptoms. The diagnostic criteria are based on two consecutive urine cultures in women and one positive culture in men (Schmiemann et al., 2010). Unlike asymptomatic UTIs, which involve bacterial growth along with underlying inflammation indicating true infection, asymptomatic bacteriuria consists of bacterial colonization without an inflammatory response and typically does not require treatment.

Recognizing the spectrum of symptoms from asymptomatic bacteriuria to severe pyelonephritis is essential for accurate diagnosis, appropriate treatment, and prevention of complications.

Diagnosis is based on clinical symptoms and confirmation of the pathogen in urine culture. Treatment generally includes antibiotics, with the choice depending on pathogen susceptibility. Increasing antimicrobial resistance emphasizes the need for cautious antibiotic use and exploration of alternative therapies.

1.3 Solitary chemosensory epithelial cells

1.3.1 Discovery of the “brush cell”

The first description of a so-called “brush cell” in the rat tracheal epithelium was provided in 1956 by Johannes Rhodin and Tore Dalhamn, based purely on ultrastructural observations using transmission electron microscopy (Rhodin and Dalhamn 1956). They identified a rare, specialized epithelial cell that, unlike ciliated epithelial cells, exhibited distinctive brush-like processes on its apical surface. Due to

this unique morphology, the newly identified, bottle-shaped epithelial cell type was termed the “brush cell.”

Following this initial finding in the trachea, similar cell types were subsequently identified in multiple organs and collectively grouped under the umbrella term solitary chemosensory epithelial cells. However, the nomenclature has varied across organs, reflecting differences in morphology and discovery context. For example, in the upper respiratory tract, these cells are most often referred to as solitary chemosensory cells (SCCs), while in the intestine, their characteristic tuft of short apical microvilli has led to the widely adopted term tuft cells (Gulbransen et al., 2008a; Gerbe et al., 2012).

Solitary chemosensory epithelial cells are distinguished from surrounding epithelial cells by their apical tuft of short microvilli and have been identified in diverse tissues across the body (Figure 1.3). These include the trachea (Rhodin and Dalhamn 1956), intestine (Höfer et al., 1996), gallbladder (Luciano and Reale 1997), stomach and pancreatic duct (Höfer and Drenckhahn 1998), taste buds of the tongue (Sbarbati et al., 1998), nasal cavity (Finger et al., 2003), vomeronasal organ (Ogura et al., 2010), tuba auditiva (Krasteva et al., 2012), urethra (Deckmann et al., 2014), thymus (Panneck et al., 2014), conjunctiva (Wiederhold et al., 2015), and gingival junctional epithelium (Zheng et al., 2019).

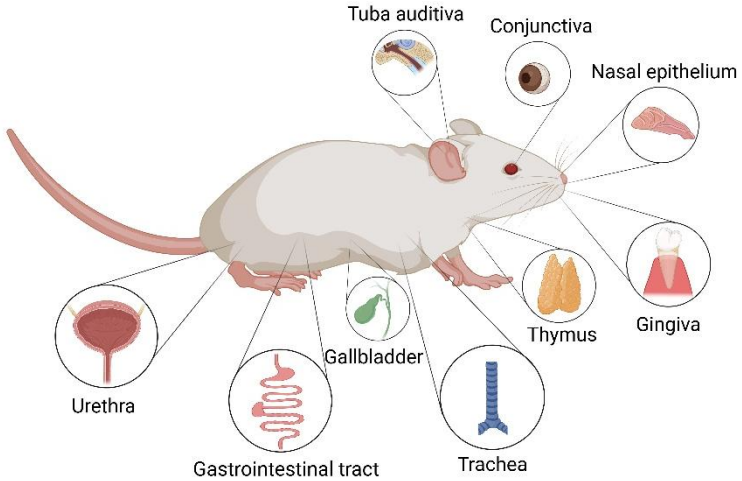

Figure 1.3: Overview of the occurrence of solitary chemosensory epithelial cells in the mouse. Created with BioRender.

1.3.2 Characterization of solitary chemosensory epithelial cells

Key components of the classical taste transduction cascade have been identified in solitary chemosensory epithelial cells, such as tuft cells of the gastrointestinal tract and SCCs of the respiratory tract (Höfer et al., 1996; Finger et al., 2003; Kaske et al., 2007;

Krasteva et al., 2011). A central element of this cascade is the transient receptor potential cation channel subfamily M member 5 (TRPM5) ion channel, which is essential for the transduction of bitter, sweet, and umami taste modalities (Zhang et al., 2003). Notably, the TRPM5 pathway can also be activated by ligands that do not bind directly to taste receptors. Examples include succinate, which binds to the succinate receptor SUCNR1 (Nadjsombati et al., 2018), and bacterial formyl peptides associated with virulence, whose receptor remains unidentified (Perniss et al., 2020).

In homozygous *Trpm5* knockout (*Trpm5*-KO) animals, taste signal transduction is disrupted across all tissues utilizing the canonical taste transduction cascade, including oropharyngeal taste buds (Zhang et al., 2003) and solitary chemosensory cells, even when signaling is initiated through non-taste receptors such as SUCNR1 (Nadjsombati et al., 2018; Perniss et al., 2023). The perception of umami, bitter, and sweet is markedly reduced but not entirely absent, suggesting the existence of TRPM5-independent signaling pathways (Damak et al., 2006). In contrast, salty and sour tastes remain unaffected. *Trpm5*-KO mice are therefore widely used as models in studies of taste and chemosensory biology (Riera et al., 2009).

In SCCs of the nasal epithelium, inhibition of PLCβ2 (phospholipase C isoform β2, located upstream of TRPM5 in the taste transduction cascade) (Lee et al., 2014) or TRPM5 attenuates intracellular calcium [Ca^{2+}] responses to denatonium, a bitter ligand for human TAS2R4 (mouse counterparts: Tas2r108 and Tas2r118) and TAS2R10 (mouse counterparts: Tas2r135, Tas2r137, or Tas2r143) receptors (Gulbransen et al., 2008b; Ogura et al., 2010) mouse: (Adler et al., 2000; Shi 2003; Meyerhof et al., 2010). Expression of TRPM5-positive chemosensory cells requires the POU homeodomain transcription factor Skn-1a/Pou2f3. Mice with genetic deletion of this factor lack these cells in all organs, including the trachea, auditory tube, nose, urethra, thymus, pancreatic duct, stomach, and large intestine (Ohmoto et al., 2013; Gerbe et al. 2016; Yamashita et al., 2017; Ndjim et al., 2024).

1.3.3 Cholinergic character of solitary chemosensory epithelial cells

Acetylcholine was first identified as a neurotransmitter by Otto Loewi in 1921, who referred to it as “Vagusstoff” (Loewi 1921). Later, Henry H. Dale established that this

substance was in fact acetylcholine, a discovery for which both scientists were jointly awarded the 1936 Nobel Prize in Physiology or Medicine (Dale 1906).

Acetylcholine is synthesized and released by both neuronal and non-neuronal cells. It acts on nicotinic and muscarinic acetylcholine receptors (nAChRs and mAChRs). Nicotinic receptors are pentameric ligand-gated ion channels composed of five subunits, which can assemble into multiple isoforms. Neuronally, acetylcholine functions as a classical neurotransmitter, mediating neuromuscular transmission at the motor end plate and acting as a neurotransmitter and neuromodulator in the central and peripheral nervous systems. Non-neuronal acetylcholine is produced by various epithelial cell types across multiple organ systems, including solitary cholinergic chemosensory cells (CCCs) (Kummer et al., 2008; Wolf-Johnston 2012; Bader et al., 2014; Kummer and Krasteva-Christ 2014; Bankova et al., 2018).

In CCCs of the trachea, nasal epithelium, vomeronasal organ, and urogenital tract, acetylcholine has been implicated in both autocrine and paracrine signaling pathways (Ogura et al., 2010; Krasteva et al., 2011; Saunders et al., 2014; Deckmann et al., 2018; Perniss et al., 2020). For instance, Saunders and colleagues (2014) demonstrated that activation of nasal SCCs leads to acetylcholine release, which stimulates nAChR on trigeminal nerve fibers, thereby triggering neurogenic inflammation in the nasal epithelium. Pharmacological inhibition with the nAChR antagonist mecamylamine (3–6 mg/kg, i.p.) significantly reduced this inflammatory response, whereas atropine, a muscarinic receptor antagonist, had no effect. This indicates that nicotinic, rather than muscarinic receptors, mediate SCC-induced neurogenic inflammation in the nasal epithelium. Accordingly, close apposition of sensory nerve fibers expressing α3 subunit (nAChRα3) to CCCs has been noted in the trachea (Krasteva et al., 2011) and in the urethra (Deckmann et al., 2014; Schmidt et al., 2025).

1.3.4 Sentinel function and defense mechanisms of extra-urethral solitary chemosensory epithelial cells

For a long time, the function of SCCs, also known as brush cells, remained unclear. More recent studies, however, have highlighted their role in infection-protective defense mechanisms, positioning them as epithelial sentinels.

Introduction

In the upper respiratory tract, stimulation of SCCs by bitter receptor ligands has been shown to trigger reflexive protective responses mediated via the trigeminal nerve. For example, inhalation of the bitter compound denatonium or N-acyl-homoserine lactones (quorum-sensing molecules produced by *Pseudomonas aeruginosa*) caused a reduction in respiratory rate in experimental animals. This response, first described by Marco Tizzano and colleagues, represents a defense mechanism that limits the absorption of harmful or toxic substances (Tizzano et al., 2010). In the lower respiratory tract, tracheal CCC that are connected to vagal sensory fibers can initiate a similar response (Krasteva et al., 2011).

Other SCC-driven protective mechanisms include the activation of ciliated epithelial cells. In the mouse trachea, CCCs respond to bacterial formyl peptides by releasing acetylcholine, which acts on M3 muscarinic receptors of neighboring ciliated cells. This results in an increased ciliary beat frequency and enhanced mucociliary clearance, thereby promoting removal of bacteria and inhaled toxins (Perniss et al., 2020). A similar phenomenon has also been observed in primary human cells. Studies using cell cultures derived from the lower respiratory tract demonstrated a direct effect on ciliated cells, where stimulation of bitter taste receptors (e.g., with denatonium) enhanced ciliary activity, thereby promoting faster clearance of harmful substances (Shah et al., 2009).

In the intestine, tuft cells (the term used for SCCs in the gut) play an essential role in immune defense. Upon infection with intestinal parasites such as helminths or the protozoan *Tritrichomonas muris*, tuft cells act as the primary source of interleukin-25 (IL-25). IL-25 activates type 2 innate lymphoid cells (ILC2s), which subsequently produce interleukin-13 (IL-13). IL-13 drives tuft cell expansion and strengthens type 2 immune responses, forming a positive feedback loop that promotes parasite clearance. In contrast, *Trpm5*-KO mice, which lack functional tuft cells, exhibit impaired parasite elimination, as shown by higher worm burdens following *Nippostrongylus brasiliensis* infection (Howitt et al., 2016; Drurey et al., 2022).

Evidence for a regeneration role of SCCs has been observed in viral infection models. In mice experimentally infected with influenza A, SCC numbers in the lungs increased significantly, peaking around day 25 post-infection, whereas uninfected control animals had no detectable SCCs in the alveolar region. Functional studies showed that intratracheal stimulation with denatonium or succinate induced plasma extravasation,

a hallmark of inflammation, in infected lungs. Repeated stimulation further increased SCC numbers, suggesting a positive feedback mechanism similar to that observed in the intestine (Rane et al., 2019).

Protective roles for SCCs have also been demonstrated in the nasal epithelium and vomeronasal organ. Genetic deletion or inhibition of TRPM5 disrupted SCC function and allowed greater penetration of bitter substances into the vomeronasal organ (Ogura et al., 2010). Similarly, mice lacking TRPM5 or Gα-gustducin, a G protein of the taste transduction cascade (McLaughlin et al., 1992), failed to exhibit protective reflexes such as reduced respiratory rate or neurogenic inflammation in response to bitter compounds defenses that were intact in wild-type animals (Tizzano et al., 2010; Saunders et al., 2014). Importantly, Saunders and colleagues demonstrated that SCC stimulation by bitter ligands or bacterial metabolites leads to acetylcholine release and subsequent activation of peptidergic nociceptive fibers, causing local neurogenic inflammation in the epithelium, which represents an additional line of mucosal defense.

Taken together, evidence from the respiratory and gastrointestinal systems demonstrates that solitary chemosensory epithelial cells act as epithelial sentinels, detecting harmful microbial metabolites or toxins and initiating rapid protective responses ranging from activation of protective neural reflexes and mucociliary clearance to immune cell recruitment and neurogenic inflammation. These findings strongly suggest that SCCs are not merely structural variants of epithelial cells but active participants in mucosal host defense. Given their presence in the urethra and urogenital tract, it is plausible that urethral SCCs fulfill similar protective functions in urinary tract defense, contributing to the early detection of pathogens and modulation of the local immune response during infection.

1.3.5 The urethral cholinergic chemosensory cell

The urethral “brush cell” was first described by our research group in 2014 using *Chat*-eGFP mice. In these animals, the gene encoding enhanced green fluorescent protein (eGFP) is expressed under the control of the choline acetyltransferase (ChAT) promoter, the enzyme responsible for acetylcholine synthesis. Microscopic examination revealed solitary *Chat*-eGFP–positive cells within the urethral epithelium and the ducts of urethral glands, while no positive cells were detected in more proximal parts of the urogenital tract, such as the bladder, ureter, or renal pelvis (Deckmann et al., 2014). This distribution pattern is consistent with that of SCCs in the airways, where

cell density decreases with increasing distance from the body's external openings (Tizzano et al., 2011; Mahmoud et al., 2025).

Immunohistochemical studies identified three distinct subpopulations of chemosensory cells in the urethra:

1. Type 1 urethral brush cells, immunoreactive for villin, ChAT, and TRPM5, further subdivided into type 1a (without PLCβ2 expression) and type 1b (with PLCβ2 expression).
2. Type 2 brush cells, immunoreactive for villin but lacking ChAT.
3. Neuroendocrine cells, producing serotonin and expressing chromogranin A and protein gene product 9.5 (Vittoria et al., 1990; Deckmann et al., 2014).

For better classification, the type 1 brush cells which synthesize and release acetylcholine were designated urethral cholinergic chemosensory cells (UCCCs). They are now called urethral tuft cells (UTC). Earlier studies in the urogenital tract using antibodies against brush cell structural proteins failed to detect these cells, likely because the urethra had not been examined at that time (Höfer and Drenckhahn 1992).

To date, UTCs have been identified in 11 mammalian species across five genera, including mouse, rat, hamster, guinea pig, monkey, human, dog, cat, badger, pig, deer, cow, and horse. Phylogenetic analyses suggest that these cells evolved at least 64.5 million years ago (Deckmann et al., 2015).

Morphologically, UTCs vary considerably and do not always display the classic bottle-shaped appearance typical of brush cells. Some possess a broad basal attachment to the basement membrane and a short apical projection into the urethral lumen, while others extend into the lumen through a narrow, tapering process. However, nearly all UTCs share immunoreactivity for the structural protein villin (Deckmann et al., 2014). Later studies have demonstrated that villin immunoreactivity may, in some cases, result from cross-reactivity of the antibody with advillin rather than from villin itself (Mahmoud et al., 2025).

Several elements of the canonical taste transduction cascade have been identified in UTCs, including α-gustducin, PLCβ2, and TRPM5 (Figure 1.4). RT-PCR confirmed the expression of the bitter receptor Tas2r108 and the umami receptor complex Tas1r1/Tas1r3, which forms a functional heterodimer (Deckmann et al., 2014). The

potent bitter compound denatonium, a known ligand for human bitter receptors TAS2R4, TAS2R8, TAS2R10, TAS2R13, TAS2R39, TAS2R43, TAS2R46, and TAS2R47 (Meyerhof et al., 2010), activates the mouse bitter receptors Tas2r108, Tas2r105, Tas2r123, Tas2r135, Tas2r140, and Tas2r144 (Chandrashekar et al., 2000; Lossow et al., 2016). Studies on dissociated UTCs revealed that exposure to denatonium (2.5–25 mM) induces a rise in intracellular calcium concentration $[Ca^{2+}]_i$. Similar increases in $[Ca^{2+}]_i$ were observed in response to monosodium glutamate (25 mM), ATP (0.5 mM), and heat-inactivated UPEC (strain CFT037, 2–5 × 10^7 CFU) (Deckmann et al., 2014).

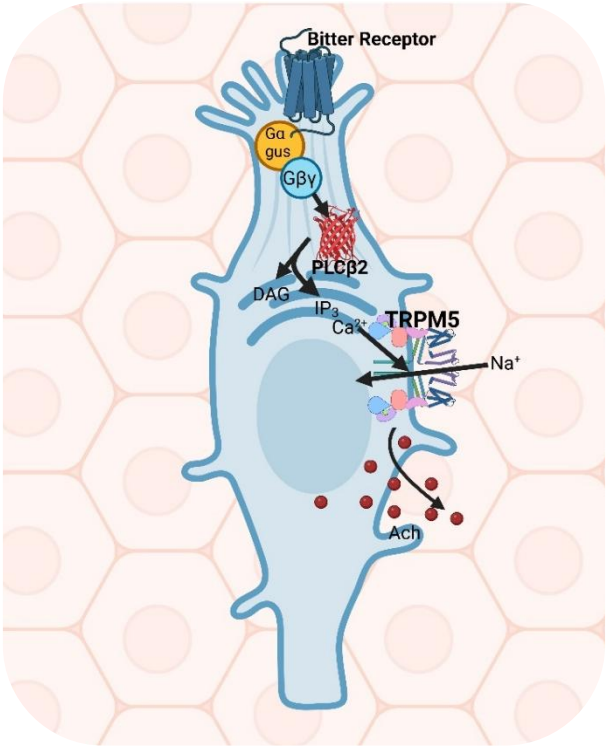

Figure 1.4: Schematic representation of the urethral cholinergic chemosensory cell). Ga gus. = gustducin, (Gαgus), gβγ = G beta-gamma complex, IP_3 = inositol 1,4,5-triphosphate**,** PLCβ2 = phospholipase C β2, DAG = diacylglycerol, TRPM5 = transient receptor potential cation channel, subfamily M, member 5, ACh = acetylcholine. Created with BioRender.

Subsequent functional studies confirmed the cholinergic nature of UTCs. Stimulation with denatonium (5 mM, 5 min) significantly increased the acetylcholine concentration in the cell supernatant compared to PBS controls. Neighboring non-chemosensory cells responded to denatonium only when located in close proximity to UTCs. These adjacent cells possess acetylcholine receptors and showed an increase in $[Ca^{2+}]_i$ upon stimulation with acetylcholine (25 µM) in presence of the acetylcholinesterase inhibitor physostigmine (5 µM). This suggests that UTCs release acetylcholine, which binds to receptors on neighboring epithelial cells to trigger calcium signaling. When cholinergic

receptor antagonists (mecamylamine 20 µM and atropine 2 µM) were applied, UTCs still responded to denatonium, but neighboring cells showed no reaction (Deckmann et al., 2014).

Beneath the urothelium, a dense network of nerve fibers can be visualized in *nAChRα3*-eGFP reporter mice, in which green fluorescence is driven by the promoter of the nicotinic acetylcholine receptor subunit α3 (nAChRα3, gene name: *chrna3*). Some of these nerve fibers extend into close proximity to UTCs (Deckmann et al., 2014). The nAChR α3 subunit is the predominant subunit expressed in viscerosensory neurons, also found in bladder-specific afferent neurons (Nandigama et al., 2013).

Further evidence for the signaling role of acetylcholine in UTCs was provided by functional experiments in rats. Deckmann and colleagues demonstrated a reflex coupling between urethral bitter stimulation and increased detrusor activity. Intraurethral application of denatonium (25 mM, 50 µL) via the ostium urethrae externum triggered detrusor contractions, resulting in rapid urethral flushing. This response was significantly reduced, though not abolished, by the nicotinic receptor blocker mecamylamine (100 µM), indicating a UTC-mediated defense reflex (Deckmann et al., 2014). Subsequent studies revealed that M2 and M5 muscarinic receptors provide negative autocrine feedback, modulating UTC activation (Deckmann et al., 2018).

UTCs function as polymodal chemosensors, co-expressing Tas1r (umami) and Tas2r (bitter) receptors, unlike type II taste cells of the tongue, which segregate these modalities (Adler et al., 2000; Ohmoto et al., 2008). This dual receptor expression likely reflects the contrasting physiological roles of these stimuli in the oral cavity: bitter tastes evoke avoidance behavior, while umami promotes nutrient intake (Briand and Salles 2016). In the urethral lumen, however, both bitter and umami ligands represent as negative signals, indicative of potential microbial presence.

Ligands of urethral bitter receptors include bacterial quorum-sensing molecules such as N-acyl-homoserine lactones, produced by *Pseudomonas aeruginosa*, a major cause of catheter-associated UTIs (Shuman and Chenoweth 2010; Maurer et al., 2015). Similarly, increased glutamate dehydrogenase expression in *Proteus mirabilis* correlates with greater pathogenicity in murine UTI models (Pearson et al., 2011), while elevated free amino acid concentrations (including umami ligands) enhance bacterial

growth (Aubron et al., 2012). These findings underscore that detection of umami compounds in the urethral lumen serves as a warning signal rather than a positive cue.

Moreover, UTCs also respond to ligands associated with other taste modalities. Exposure to sodium chloride (50–150 mM) induced an increase in $[Ca^{2+}]_i$ via activation of the epithelial sodium channel (ENaC), suggesting that UTCs can also sense salt stimuli (Kandel et al., 2018).

1.4 Urethral innervation

1.4.1 Sensory innervation

The urethra receives a complex innervation including autonomic (sympathetic and parasympathetic) visceromotor (= visceroefferent) fibers, somatomotor fibers to the striated muscles of the sphincter complex, and sensory (= afferent) fibers (de Groat et al., 2015; Ferreira and Duarte Cruz 2021). Among these, the sensory innervation is of particular interest in the context of the present work.

The pseudounipolar neuronal cell bodies of urethral afferents are located in lumbosacral the dorsal root ganglia (DRG). Their axons reach the lower urinary tract (LUT) via the hypogastric, pelvic and pudendal nerves. Functionally, they include myelinated, fast conducting A-fibers and unmyelinated, slow conducting C-fibers. Lumbar splanchnic nerves, lumbar white rami and hypogastric nerves showed activity of different fibers including small myelinated Aδ- and unmyelinated C-fibers (Winter 1971; Floyd et al., 1976; Bahns et al., 1986). Single or multiple punctuate regions represent the receptive fields on the bladder or urethral surface or have connections with the blood vessels in the peritoneum attached to the bladder base. The afferents respond at intravesical pressures from 10 to 70 mmHg in a graded manner. The afferents from the urethra show either no responses to a bladder excitation or low response at high intravesical pressures. Even though the Aδ- and C-fiber afferent populations are similar, the firing rates were lower in the C-fibers. The hypogastric afferents are in the active status when the bladder is empty and this is in contrast to pelvic nerves (de Groat et al., 2015).

In dogs, urethral afferents in the pudendal and pelvic nerves are sensitive to fluid passing through the urethra, with pudendal nerve afferents being more sensitive than pelvic nerve afferents. Moreover, high intraurethral pressures (>60 cm water) activates rat pelvic nerve afferents (Feber et al., 1998; de Groat et al. 2015).

Introduction

In cat, the conduction velocities of pudendal nerve afferent fibers are twice as fast (40 m/s versus 25 m/s) as the pelvic nerve afferent fibers affected by the same stimulus, being in the Aβ range (Bradley et al 1973). Moreover, the fibers in the pudendal, pelvic and hypogastric nerves show variable receptor criteria. Pudendal nerve afferents showed a very slow adaptation pattern in response to urine flow. On the other hand, small myelinated or unmyelinated afferents in the hypogastric nerve and those with myelin in the pelvic nerves respond to urine flow or the distension of urethra showing fast adaptation. Intraurethral saline infusion stimulates the flow sensing urethral afferents and, thereby, increase volume-induced reflex contraction of the bladder of rat (Jung et al., 1999). Reflex bladder contractions were also evoked by electrical stimulation of urethral afferents in cat (Kennelly et al., 2010; Kennelly et al., 2011; McGee 2014; de Groat et al. 2015). Chemically, such reflex bladder contraction with enhanced micturition frequency can be evoked by intraurethral application of the bitter substance, denatonium, which is an activator of UTCs (Deckmann et al., 2014). Involvement of UTCs as the initial sensor in this reflex is further supported by the findings that a) UTCs release acetylcholine in response to denatonium, b) they are approached by sensory fibers expressing the cholinergic receptor subunit nAChRα3, and c) the nAChR inhibitor mecamylamine largely suppresses the reflex response. This urethra-to-bladder reflex is interpreted as a protective mechanism by inducing flushing of the urethra when potentially hazardous compounds are detected on the mucosal surface by UTCs (Deckmann et al., 2014).

In addition, the pelvic and pudendal nerves innervating the urethra have nociceptive C-fiber afferents, with more of them running in the pelvic than in the pudendal nerves. In humans, these afferent fibers travel mainly through the pelvic and pudendal nerves. Their cell bodies are situated in the sacral DRG at the S2–S4 spinal levels. In the rat, L6–S1 DRG provide rich sensory innervation to the urethra (Yoshimura et al., 2003). Application of capsaicin, the pungent ingredient of hot chili pepper, stimulates urethral C-fibers, which leads to activation of the external urethral sphincter and increase in pelvic floor striated muscle electromyography (EMG) activity, and to nociceptive behavioral responses, which are masked after the transection of pudendal nerve. The activation of urethral C-fibers by capsaicin initially activates and then inhibits bladder contractions in rats. The subepithelium, submucosa, and muscular layers in each part of the urethra have putative C-fiber afferent fibers that can be identified by positive immunostaining for the neuropeptides calcitonin gene-related peptide (CGRP) or

substance P (SP) (de Groat et al. 2015), which are key mediators of the so-called neurogenic inflammation, a local defense reaction driven by peptidergic sensory nerve fibers.

1.4.2 Neurogenic inflammation

Inflammation represents the body's response to harmful stimuli and has been classically characterized by the five cardinal signs: swelling (tumor), heat (calor), redness (rubor), pain (dolor), and loss of function (functio laesa) (Rather 1971).

Nociceptors, the free sensory nerve endings that detect tissue damage, play a central role in neurogenic inflammation. They are activated by noxious external stimuli such as high heat (>45 °C), strong mechanical stress, chemical irritants, electrical stimuli, or UV radiation (Dubin and Patapoutian 2010). Once activated, nociceptors generate action potentials that are transmitted to the dorsal horn of the spinal cord via myelinated group III (Aδ) fibers or unmyelinated group IV (C) fibers. A subpopulation of nociceptors produces neuropeptides of the tachykinin family, mainly SP, and often CGRP in addition. These peptidergic sensory fibers serve a dual function. In addition to transmitting information towards the CNS - the classical sensory function - they release these neuropeptides from their peripheral ending, which evokes a local response, the so-called local effector function (Holzer 1994). While action potentials are transmitted orthodromically toward the spinal cord, they also enter axon collaterals that have not been excited by the initial stimulus and, there, propagate antidromically into their peripheral endings. This antidromic signaling leads to the local release of neuropeptides also from those peripheral nerve endings of the same neuron, which were not initially excited. The neuropeptides initiate an inflammatory reaction in the surrounding tissue a process termed neurogenic inflammation (Holzer 1988). (Figure 1.5).

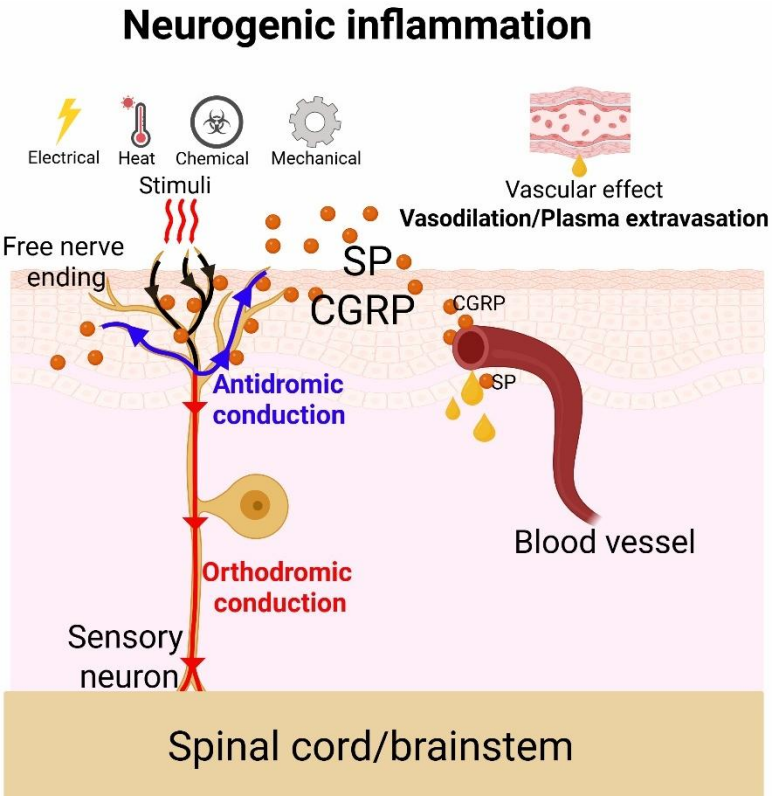

Figure 1.5: Schematic representation of stimulus conduction following noxious activation of free nerve endings. Pain perception occurs through orthodromic transmission via the dorsal root to the dorsal horn of the spinal cord. Simultaneously, antidromic conduction releases neuropeptides from axonal varicosities outside the initial site of stimulation, resulting in a localized inflammatory response. Created with BioRender.

Chemical stimuli such as capsaicin (from chili peppers) and mustard oil exemplify this mechanism. Capsaicin acts as an agonist of transient receptor potential vanilloid TRPV1 channels (Caterina et al. 1997), while mustard oil activates TRPV1 and TRPA1 (transient receptor potential cation channel subfamily A member 1) channels (Everaerts et al. 2011). These channels mediate the excitability of nociceptors. Early work by Bruce (1910, 1913) showed that mustard oil induces vasodilation in the skin through a nerve-dependent mechanism, which he attributed to the axon reflex, where antidromic action potentials spread inflammation beyond the site of initial irritation.

Thomas Lewis (1927) described the classical “triple response” of neurogenic inflammation: (1) a red line at the site of mechanical irritation, (2) a surrounding flare (erythema), and (3) linear edema — responses reproduced in modern experiments (Figure 1.6).

Figure 1.6: Neurogenic inflammation of the skin induced by a noxious mechanical stimulus. A blunt plastic pin was drawn across the inner forearm. (**a**) The erythema extends beyond the original site of irritation. (**b**) After 5 min, a linear edema develops. Illustration recreated after Lewis (1927).

The two hallmark features of neurogenic inflammation are plasma extravasation and vasodilation. These are mediated primarily by the neuropeptides SP and CGRP, which are produced in sensory neurons and transported in axons to their peripheral endings (Holzer 1998).

- Vasodilation results mainly from CGRP release at axonal varicosities. CGRP binds to receptors on vascular smooth muscle cells, leading to arteriolar dilation and increased blood flow (hyperemia).
- Plasma extravasation is mediated largely by SP and neurokinin A, a structurally related tachykinin, in the early phase, which act on postcapillary venules to increase endothelial permeability, allowing plasma leakage into surrounding tissue (Holzer 1998).

Introduction

Neuropeptide signaling is frequency-dependent: vasodilation can be triggered even by low-frequency stimulation (~0.025 Hz), whereas plasma extravasation requires higher-frequency activation (>2 Hz) (Holzer 1992).

SP was identified by Lembeck (1953) as the mediator of plasma extravasation. It binds to neurokinin receptors (NK1R, NK2R, NK3R) with varying affinities (Mantyh 2002), among which NK1R is primarily responsible for plasma extravasation (Devor et al., 1989). The peptide CGRP, a 37–amino acid molecule existing in α and β isoforms, binds to a receptor complex consisting of the calcitonin-like receptor (CLR), receptor activity-modifying protein 1 (RAMP1), and receptor component protein (RCP) (McLatchie et al., 1998). CGRP strongly potentiates SP-induced plasma extravasation, as demonstrated in rat trachea and skin models (Brokaw and White 1992; Chu et al., 2000; Sawyer et al., 2011). This potentiation may result from increased local blood flow ("two mediator hypothesis"; (Williams and Morley 1973) or reduced enzymatic degradation of SP (Le Grevès et al., 1989).

Importantly, receptors for SP and CGRP are also expressed on immune cells including mast cells, dendritic cells, and T lymphocytes (Hosoi et al., 1993; Ding et al., 2008; Cyphert et al., 2009; Mikami et al., 2011; Rochlitzer et al., 2011). Thus, neurogenic inflammation not only influences the vascular system but also modulates innate and adaptive immunity. SP and CGRP have been implicated in wound healing (Brain 1997) and inflammatory disease models. For example, intra-articular SP injection worsened inflammation in rat arthritis models, while denervation reduced it (Levine et al., 1984).

This close interplay between neuropeptides and immune cells suggests that dysregulated neurogenic inflammation contributes to immune maladaptations, including allergic reactions and autoimmune diseases (Caceres et al., 2009; Ostrowski et al., 2011).

Taken together, neurogenic inflammation represents a highly dynamic process in which nociceptor activation leads to the release of neuropeptides such as SP and CGRP, driving vasodilation, plasma extravasation, and immune cell recruitment. Beyond their vascular and immune effects, these pathways are increasingly recognized as part of the epithelial defense system, since specialized epithelial cells such as solitary chemosensory epithelial cells can activate nearby sensory nerves and trigger neurogenic inflammation (Hollenhorst and Krasteva-Christ 2023). This positions SCCs

as key modulators at the interface between epithelial sensing and neural-immune communication.

1.5 Aims of the work

Brush cells are specialized epithelial sensors that detect hazardous substances. Upon activation, they release acetylcholine and other mediators, which in turn stimulate various target cells, including immune cells and nearby sensory nerve fibers (Schneider 2021; Strine and Wilen 2022). In the nose and trachea, activation of these fibers results in the release of SP, leading to neurogenic inflammation (Saunders et al., 2014; Hollenhorst et al., 2022).

Previous work in our lab showed that denatonium induced SP release in the urethra. (Schmidt 2021), indicating that initiation of a neurogenic inflammation might also belong to the repertoire of defense reactions triggered by UCCCs. However, denatonium is not a cell type-specific stimulus, which selectively activates only brush cells, but can broadly activate multiple cell types as it has been shown in the rat trachea (Lasconi et al., 2019). The present study, therefore, aims to elucidate the contribution of urethral brush cells to neurogenic inflammation in the urethra by a) establishing a model for the selective activation of brush cells, and b) utilizing a model of brush cell-deficient mice. Neuropeptide release from explanted mouse urethrae subjected to various stimuli was taken as readout for the initiation of neurogenic inflammation.

To achieve selective activation of brush cells, two complementary approaches were employed:

1. Optogenetic model: A transgenic mouse line (*Chat-ChR2-EYFP*) expressing a fusion protein of the blue light-sensitive ion channel channelrhodopsin-2 (ChR2) and enhanced yellow fluorescent protein (EYFP) under the control of the *Chat* promoter. Here, explanted urethrae were stimulated with blue LED light.
2. Chemogenetic model: Mice expressing a designer receptor exclusively activated by designer drugs (DREADD) under the control of the *Trpm5* promoter, a brush cell-specific cation channel. Here, explanted urethrae were stimulated with the selective DREADD ligand CNO (clozapine N-oxide). DREADDs are modified receptors that respond only to a synthetic, otherwise inert compound rather than to the body's natural neurotransmitters. CNO serves as this synthetic

activator; it binds specifically to DREADDs and turns the engineered cells “on” or “off,” allowing researchers to control cellular activity with high precision in living tissue (Urban and Roth 2015).

As third model, mice lacking brush cells due to genetic deletion of the transcription factor Pou2f3 (*Pou2f3*$^{-/-}$) were employed. Here, explanted urethrae were stimulated with denatonium.

In this way, the study seeks to clarify whether brush cells directly contribute to neurogenic inflammation in the urethra and to define their role in the local host defense response.

2. Materials and methods

2.1 Animals

2.1.1 Mouse strains

The experimental animals were kept and bred in the central animal facilities of the Justus Liebig University (JLU) in Giessen (approval numbers of the Institutional Animal Care 571_M, 641_M, 793_M and 741_M), the Philipps University of Marburg (Ex-1-2020 and AK-1-2023) and University of Saarland School of Medicine Homburg/Saar (CIPMM-2.2.4.1.1) at specific-pathogen free conditions. More details about these mice are listed in Table 2.1. All animals were kept in individually ventilated cages, with access to food and water ad libitum, and a light-dark cycle of 14 hours light and 10 hours dark except for mice kept in Homburg with a light-dark cycle of 12 hours light and 12 hours dark.

C57BL/6JRj

C57BL/6JRj mice were purchased from Charles River Laboratories (Wilmington, USA) and Janvier Labs (Janvier Laboratories, Le Genest Saint Isle, France) and kept at the JLU. A total of 12 C57BL/6JRj mice (12 females) between the ages of 18 and 31 weeks were used.

ChAT-ChR2-EYFP

*B6.Cg-Tg(Chat-COP4*H134R/EYFP, Slc18a3)6Gfng/J* mice, common name: *Chat-ChR2-EYFP* (RRID: IMSR_JAX:014546) shall express a fusion protein of channelrhodopsin-2 (ChR2) and enhanced yellow fluorescent protein (EYFP) under the control of the choline acetyltransferase (*Chat*) promotor. Previously, we used this strain successfully to study tracheal and gall bladder tuft cell function (Perniss et al. 2020; Keshavarz et al., 2022). *Chat-ChR2-EYFP* mice were obtained from Jackson Laboratories, stock nr. 014546. The animal protocols are Ex-1-2020 and AK-1-2023). A total of 26 *Chat-ChR2-EYFP* transgenic (12 females, 14 males) and 11 *Chat-ChR2-EYFP* control mice (4 females, 7 males) between the ages of 17 and 31 weeks was used.

Pou2f3

B6.129-Pou2f3^{tm1Abek} mice, common name *Pou2f3*$^{-/-}$, were obtained from I. Matsumoto, Monell Chemical Senses Center, Philadelphia, PA, USA, and kept and bred at the JLU. These mice were characterized previously (Matsumoto et al., 2011, Yamashita et al., 2017). A total of 13 *Pou2f3*$^{+/+}$ mice (3 females, 10 males) and 13 *Pou2f3*$^{-/-}$ *mice* (4 females, 9 males) between the ages of 17 and 31 weeks were used.

Trpm5-DREADD

Trpm5-DREADD mice were generated previously by crossing *Trpm5*-IRES-Cre and Rosa26-NLSiRFP720-2A-Gq (DREADD) knock-in mice (Yu et al., 2023). They were provided by U, Boehm, Experimental Pharmacology, Center for Molecular Signaling, Saarland University, Homburg, Germany. This strain was characterized previously (Yu et al., 2023). A total of 16 *Trpm5-DREADD* mice (8 females, 8 males) and 16 Rosa26-NLSiRFP720-2A-Gq (DREADD) knockin mice (8 females, 8 males) between the ages of 17 and 31 weeks were used.

Mouse strain name	**Abbreviated name**	**Original source**	**Reference**
C57BL/6JRj	BL6	Janvier Labs	N/A
B6.Cg-Tg(Chat-COP4*H134R/EYFP,8a3)6Gfng/J (Chat-ChR2-EYFP)	ChAT-ChR2-EYFP	Jackson Labs	Zhao et. al., 2011
Pou2f3^{tm1Abek}	Pou2f3	I. Matsumoto, Monell Chemical Senses Center, Philadelphia, PA, USA	Matsumoto et al., 2011
Trpm5-DREADD	Trpm5-DREADD	U. Boehm, Saarland University, Germany	Yu et al., 2023

Table 2.1: Mouse strains

2.2. Chemicals, media and reagents

The chemicals, media and reagents used are listed in Table 2.2

Substance	**Source**	**CAS No.**
Aqua dest	Sigma-Aldrich, St. Louis, USA	7732-18-5

Bovine serum albumin	Thermo Fisher Scientific, Waltham, USA	15561020
Capsaicin	Sigma-Aldrich, St. Louis, USA	404-86-4
Clozapine N-oxide (CNO)	Biotechne, Minneapolis, Minnesota, USA	34233-69-7
Denatonium benzoate	Sigma-Aldrich, St. Louis, USA	3734-33-6
Dimethylsulfoxide (DMSO)	Call Roth, Karlsruhe, Germany	67-68-5
Dinatriumhydrogenphosphate-Dihydrate	Carl Roth, Karlsruhe, Germany	10028-24-7
Disodium carbonate	Merck, Darmstadt, Germany	497-19-8
Disodium hydrogen phosphate dihydrate	Carl Roth, Karlsruhe, Germany	10028-24-7
Distilled water	B.Braun, Melsungen, Germany	7732-18-5
Dulbecco's Modified Eagles's Medium (DMEM)	Thermo Fischer Scientific, Waltham, USA	1342278-01-6
4′,6-Diamidino-2-phenylindol (DAPI)	Sigma-Aldrich, St. Louis, USA	28718-90-3
Ethanol 96%	Carl Roth, Karlsruhe, Germany	64-17-5
Formaldehyde solution (37%)	Carl Roth, Karlsruhe, Germany	50-00-0
Glycerol	Carl Roth, Karlsruhe, Germany	56-81-5
Horse serum	PAA-Laboratories, Hessen, Germany	7558-79-4
Isoflurane	Abbott, Illinois, USA	26675-46-7

Liquid nitrogen	Linde, Leuna, Germany	7727-37-9
Mecamylamine	Sigma-Aldrich, St. Louis, USA	826-39-1
2-Methylbutane	Call Roth, Karlsruhe, Germany	78-78-4
Paraformaldehyde (PFA)	Merck, Darmstadt, Germany	30525-89-4
Phosphate-buffered saline (PBS)	Thermo Fisher Scientific, Waltham, USA	Cat. # J61196.AP
Saturated picric acid	Sigma-Aldrich, St. Louis, USA	88-89-1
Sodium chloride	Carl Roth, Karlsruhe, Germany	7647-14-5
Sodium dihydrogen phosphate dihydrate	Carl Roth, Karlsruhe, Germany	13472-35-0
Sodium hydrogen carbonate	Sigma-Aldrich, St. Louis, USA	144-55-8
Sucrose	Merck, Darmstadt, Germany	57-50-1
Tissue-Tek-O.C.T.-compound	Sakura Finetek, Alphen aan den Rijn, Netherlands	Cat. # 25608-930
Tween 20	Sigma-Aldrich, St. Louis, USA	9005-64-5

Table 2.2: Chemicals, media and reagents

2.3 Formulations of solutions and buffers

The solutions and buffers used were prepared according to the instructions given in Table 2.3

Name	**Recipe**
Blocking solution	10% horse serum, 0.1% bovine serum albumin and

	0.5% Tween 20 in PBS.
Buffered glycerol	50 ml 0.5 M sodium hydrogen carbonate with 0.5 M disodium carbonate adjusted to pH 8.6. Mixed with glycerol in a ratio of 1:2.
CNO stock solution 10 mM	1 µl 60 mM CNO solved in 20 mg/ml DMSO deleted in 1000 µl PBS.
Ethanol 70%	66.5 ml ethanol 96%, 33.5 ml aqua dest.
PBS for use in immunohistochemistry	28.75 ml solution A, 96.2 ml solution B, 22.4 g sodium chloride in 5 liters distilled water. pH: 7.4.
PBS+S	PBS with additional 22.4 g sodium chloride per liter.
Phosphate buffer	0.2 M 230 ml solution A, 770 ml solution B.
Phosphate buffer 0.1 M	230 ml solution A, 770 ml solution B, 1 liter distilled water, pH: 7.4.
PFA 4%	40 g PFA, 500 ml distilled water, 500 ml of 0.2 M PP.
Solution A	31.2 g sodium dihydrogen phosphate dihydrate in 1 liter of distilled water.
Solution B	35.6 g disodium hydrogen phosphate dihydrate in 1 liter of distilled water.
Sucrose solution 18%	18 g sucrose made up to 100 ml with 0.1 M phosphate buffer.
Zamboni fixative solution	50 ml of 37% formaldehyde solution, 500 ml of 0.2 M phosphate buffer and 150 ml of saturated picric acid are mixed. The solution is made up to one liter with distilled water.

Table 2.3: The solutions and buffers

2.4 Devices

The devices listed in Table 2.4 were used.

Name	Manufacturer
Anesthesia machine UniVet Porta UV17001-T9	Groppler Medizintechnik, Deggendorf, Germany
Camera AxioCam color HR	Zeiss, Jena, Germany
Camera AxioCam monochrome MRm	Zeiss, Jena, Germany
Cryostat Microm HM 560	Thermo Fischer Scientific; Waltham, USA
Delta-T shell and stage adapter	Bioptechs, Butler, USA
Elisa reader infinite M1000 pro	Tecan, Zurich, Switzerland
Fluorescence microscope Zeiss Axioplan 2	Zeiss, Jena, Germany
Eppendorf centrifuge 5424	Eppendorf AG, Hamburg, Germany
Intas money documentation system	Intas Science Imaging Instruments GmbH, Gottingen, Germany
Intas Scientific Grad Camera	Intas Science Imaging Instruments GmbH, Gottingen, Germany
Multichannel pipette Matrix 1250µl	Thermo Fischer Scientific; Waltham, USA
Precision balance SBA 31	Scaltec Instruments GmbH, Gottingen, Germany
Shaker Edmund buhler	neoLab Migge GmbH, Heidelberg, Germany
Vibrating mill MM 400	neoLab Migge GmbH, Heidelberg, Germany

Table 2.4: Devices used

2.5 Consumables

The consumables used are listed in Table 2.5

Name	Company
Adhesion slide Superfrost Plus	R. Langenbrinck GmbH,

	Emmendingen, Germany
Cell culture multiwell plate 24 wells	Greiner Bio-One, Kremsmünster, Austria
Filter paper 42.5 mm Ø	Whatman, Maidstone, United Kingdom Kingdom
Grease pencil PAP Pen Liquid Blocker	Science Services, Munich, Germany
Parafilm	Bemis, Neenah, USA
Precision cover glasses 24 x 60 mm	Carl Roth, Karlsruhe, Germany

Table 2.5: Consumables

2.6 Software

The software programs used for the evaluation are listed in Table 2.6

Designation	**Manufacturer**
AxioVision Rel. 4.8	Zeiss
Excel	Microsoft
GraphPad Prism 6	GraphPad Software
ImageJ 1.49	(Schneider et al. 2012)
PowerPoint	Microsoft
BioRender	https://app.biorender.com

Table 2.6: Software used

2.7 Immunohistochemistry

2.7.1 Tissue preparation

2.7.1.1 Sacrifice of animals

The experimental animals were killed by anesthesia using isoflurane inhalation (0.3 ml to 1 liter vessel) and then exsanguination by cutting the abdominal aorta or by cervical dislocation.

2.7.1.2 Urethra preparation

After the animals were killed, the pelvis was cut on both sides of the pubis and the urethra was exposed. In female animals, the urethra was dissected from the underlying

vagina to the ventral pubic angle and removed together with the bladder. In the male animal, the erectile tissue of the penis was separated from the foreskin, the membranous part of the urethra was separated from surrounding accessory sex glands and dissected together with the bladder. The tissue was then separated by severing the bulbocavernosus muscle and removed together with the bladder. Dorsal root ganglia were removed from the dorsal aspect of the thoracic and lumbar region after the spinal canal was opened.

Fixation was carried out overnight by immersion in Zamboni fixative solution. The tissue samples were then washed repeatedly with 0.1 M phosphate buffer until no yellow coloration of the supernatant was evident. The tissue was shaken on a shaker during fixation and subsequent processing. The samples were immersed in an 18% sucrose solution overnight. The next day, parts of the penis containing the penis bone were removed from samples from male animals. The samples were then placed in Tissue-Tek-O.C.T.-Compound, embedded on filter paper and frozen in 2-methylbutane cooled with liquid nitrogen. The samples were stored at -20°C until further use.

2.7.2 Indirect immunofluorescence of cryosections

Ten µm thick cryostat sections were made on the cryostat at -22°C and collected on adhesion slides. Sections were air-dried for 1 h in the dark at room temperature and then either used immediately for immunohistochemistry or stored at −20°C. To prevent antibody solutions from running off, the sections were outlined with a grease pencil. One hundred µl block solution per slide was added to the sections and incubated for one hour in a dark chamber at room temperature. The blocking solution reduces non-specific antibody markings by occupying free protein binding sites. After 1 hour, the block solution was aspirated and replaced with the primary antibody solution as listed in table 2.7. The primary antibodies were added singly for immunolabeling. The primary antibodies were diluted with PBS+S to working concentration. Sections were incubated overnight in a humid parafilm-sealed chamber at room temperature.

The next day, the sections were washed twice in PBS for 10 min each and then incubated with the secondary antibody solution for 1 h as listed in table 2.8. The secondary antibodies were added singly for immunolabeling. Here too, the secondary antibodies were diluted with PBS+S to working concentration.

Antigen	Host	Dilution	Source	RRID
DCLK1	Rabbit polyclonal	1:1000	Abcam, Cambridge, UK	AB_873537
SP	Rat, monoclonal	1:400	Santa Cruz Biotechnology, Texas, USA	AB_2747414
CGRP	Goat, polyclonal	1:1600	Neo biotech, Gangwon-do, South Korea	AB_572217

Table 2.7: Primary antibodies used for immunofluorescence labeling

Antigen	Host	Conjugate	Dilution	Source	RRID
Rabbit Ig	Donkey	Cy3	1:2000	Chemicon, Limburg, Germany	AB_92588
Rat Ig	Donkey	Cy3	1:1600	Dianova, Hamburg, Germany	AB_2340667
Goat Ig	Donkey	Cy3	1:400	Dianova, Hamburg, Germany	AB_2340411

Table 2.8: Secondary antibodies used for immunofluorescence labeling

After the secondary antibody solution was aspirated, the sections were washed twice in PBS for 10 min each and then fixed in 4% PFA for 10 min. This was followed by another two ten-minute washing steps in PBS. After brief drying, buffered glycerol mixed with the fluorescent dye DAPI (4′,6-diamidino-2-phenylindole; 1 µg/ml) was used to label the nucleus and was applied to the sections and they were covered with a precision coverslip. The sections were stored in the dark at 4°C until they were evaluated.

All incubation steps were carried out in dark storage to prevent the fluorescent dyes from fading.

2.7.3 Controls

In order to test for non-specific binding of the secondary antibodies, the primary antibody solution was replaced by PBS on one slide per incubation. Moreover, murine gallbladder was used as a positive control for DCLK1 antibody.

2.7.4 Evaluation and documentation using microscopy

The evaluation and documentation were carried out on an epifluorescence microscope equipped with appropriate filter sets (Table 2.9). Immunohistochemical markings were recorded using AxioVision software. Image processing was restricted to adjusting contrast and brightness and coloring black and white images and was done using the ImageJ software.

Fluorescent dyes	Excitation filter	Dichroic mirror	Emission filter
Cy3	525-560 nm	555 nm	570-650 nm
eGFP/eYFP	460-490 nm	505 nm	515-550 nm
DAPI	360-370 nm	400 nm	420-460 nm

Table 2.9: Epifluorescence microscope filters.

2.7.5 Cell counting

For quantitative assessment of single and double-labeling immunofluorescence in sections of the urethra (DCLK1/YFP, 5 animals, 3-4 sections each with a distance of at least 50 µm from each other), counting was done manually using an Axioplan 2 epifluorescence microscope equipped with a 40× objective lens, evaluating the entire section plane. For each urethra, the total count of single and double positive cells and their percentages and average numbers were calculated.

2.8 Enzyme linked immunosorbent assay (ELISA)

The ELISA kit used was the SP ELISA-Kit from Bio-techne, Minneapolis, USA.

2.8.1 Sample collection and experimental procedure Samples from mice of the C57BL/6J, *ChAT-ChR2-EYFP*, *Pou2f3* and *Trpm5-DREADD* strains were used. The mice were killed by cervical dislocation after anesthesia using isoflurane inhalation and then exsanguinated by cutting the abdominal aorta. The urethra was removed, separated from the bladder and cut lengthwise to expose the lumen. In the male animal, the urethra was divided into two parts: part A, the penile part of the urethra, and part B, the membranous part of the urethra. The experimental procedure was carried out according to the scheme shown in Figure 2.1. The urethrae were transferred to a 24-well cell culture plate with 500 µl of DMEM culture medium. The tissue samples were then washed with 500 µl of PBS. In the first step, the samples were incubated for 10 min in 210 µl PBS, the supernatant (supernatant 1) was collected and shock-frozen in liquid nitrogen. The urethra was then stimulated in fresh PBS (210 µl) for a further 10 min in the second step with one of the following conditions: a) exposure to LED blue light, b) with mecamylamine (mecamylamine 20 µM) in the medium with exposure to LED blue light, c) denatonium (5 mM dissolved in PBS), d) capsaicin (1 mM; dissolved in PBS with 10% EtOH), e) clozapine N-oxide (CNO, 60 µM dissolved in PBS with 60 µM DMSO) or f) PBS as a negative control. The supernatant (supernatant 2) was then collected and shock-frozen. After taking the supernatants, the weights of the tissue samples were determined using a precision balance scale. The supernatants were subsequently used in the SP ELISA kit. The ELISA was carried out according to the manufacturer's instructions. A standard curve (see 2.8.2) was used to determine the concentration of unknown sample.

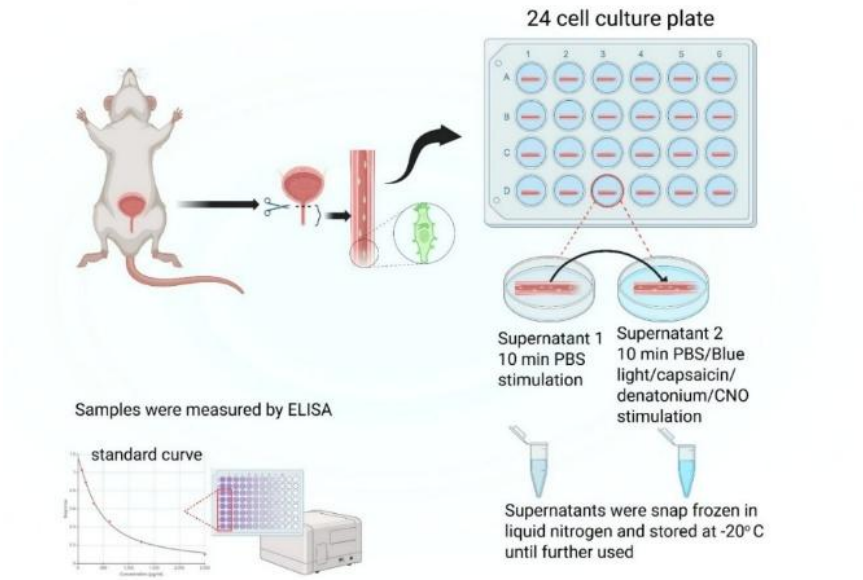

Figure 2.1: Schematic representation of sampling for use in ELISA

2.8.2 Evaluation

The subsequent colorimetric measurement was carried out using ELISA plate reader (Table 2.4). Calibration was done through a standard curve, appling synthetic SP in a concentration range from 78.1-2500 pg/ml. The detection range was 402-1576 pg/ml for SP. The standard curve was calculated using the ELISA analysis software with a 4-parameter logistic regression. Sample measurement values were interpolated using the standard curve. The determined substance concentrations in the supernatants were then related to the determined tissue weights and finally given as pg/ml/mg.

2.9 Statistics

The statistical analysis was carried out using the Prism program (version 8), as was the creation of the graphs. The schemes were created using BioRender (https://app.biorender.com). Data deviated significantly from normal distribution as shown by D'Agostino-Pearson omnibus test applied to the largest possible sample. Therefore, data were presented as median ± interquartile range (IQR), and non-parametric tests (Wilcoxon test and Mann-Whitney test) were used for statistical evaluation. The difference between two or more groups was considered statistically significant if $p < 0.05$ was present.

3 Results

3.1 CNO induces neuropeptide release from *Trpm5*-DREADD and DREADD control, but not from C57BL/6JRj urethrae

Peptidergic nerve fibers are in close proximity to UTCs, suggesting a possible functional interaction between UTCs and them (Deckmann et al., 2014; Schmidt et al. 2025). To investigate whether UTCs can induce neuropeptide release from these nerve terminals, we utilized freshly explanted urethrae, stimulated the UTCs, and measured neuropeptide levels in the supernatant. Although isolated UTCs are known to respond to various chemical stimuli (Deckmann et al. 2014; Kandel et al. 2018; Schmidt et al. 2024), this does not exclude the possibility of indirect effects due to concomitant chemical stimulation of other mucosal cell types. To stimulate UTCs directly, we employed both chemogenetic and optogenetic approaches. For the chemogenetic model, we used *Trpm5*-DREADD mice, in which the *Trpm5* promoter drives expression of a Gq-coupled DREADD. This receptor can be specifically activated by the synthetic compound CNO. Previous work showed that this model can be used to induce ATP release from tuft cells in the mouse trachea upon CNO application (Abdel Wadood et al. 2025).

Urethrae from *Trpm5*-DREADD, DREADD control and C57BL/6JRj mice were incubated for 10 min in PBS, followed by another 10 min in PBS with 60 µM CNO as a stimulus. Supernatants were collected and analyzed for SP concentration using commercial SP ELISA kits, following the manufacturer's protocol. SP levels were normalized to tissue weight.

In *Trpm5*-DREADD mice, CNO significantly increased SP concentration in the supernatant ($p=0.0001$, Wilcoxon matched-pairs signed rank test) (Figure 3.1), with a median increase of 55 pg/ml per mg of urethra. Although not carrying the designer receptor for CNO, DREADD control mice also showed a significant SP release under the same conditions ($p=0.0006$, Wilcoxon matched-pairs signed rank test) (Figure 3.1) with a median release of 43.87 pg/ml/mg of urethra compared to the PBS control. Comparing both strains, the release of SP in *Trpm5*-DREADD and DREADD control mice showed no significant difference after 10 min CNO administration ($p=0.4016$; Mann-Whitney test) (Figure 3.2).

As a further negative control, I used C57BL/6JRj mice. In this strain, CNO did not evoke an increase in SP release, with a median change of 3.972 pg/ml/mg of urethra between PBS and CNO exposure (p=0.8984, Wilcoxon matched-pairs signed rank test) (Figure 3.1). This differed significantly (p=0.0229, Mann-Whitney test) from that what was found in *Trpm5*-DREADD mice and nearly significantly (p=0.0501) from the effect seen in DREADD control mice (Figure 3.2).

In C57BL/6JRj mice, the effect of vehicle (DMSO) in which CNO was dissolved, was tested. There was no significant difference in SP concentration in supernatant taken before and after application of DMSO (p=0.7422, Wilcoxon matched-pairs signed rank test) (Figure 3.1), and there was also no significant difference when Δ-values in response to CNO and vehicle (DMSO) were compared (p=0.5999; Mann-Whitney test) (Figure 3.2).

In summary, CNO had no effect when applied to isolated urethrae from wild-type (C57BL/6J) mice (as predicted), but it did evoke the release of SP in both *Trpm5*-DREADD and DREADD control mice to a similar degree. This indicates that the model is not suitable model for studying UTC-driven neuropeptide release in our system. This outcome aligns with previous findings in the small intestine, where a DREADD-based approach also failed to produce paracrine action mediated by acetylcholine release from tuft cells (Billipp et al. 2024).

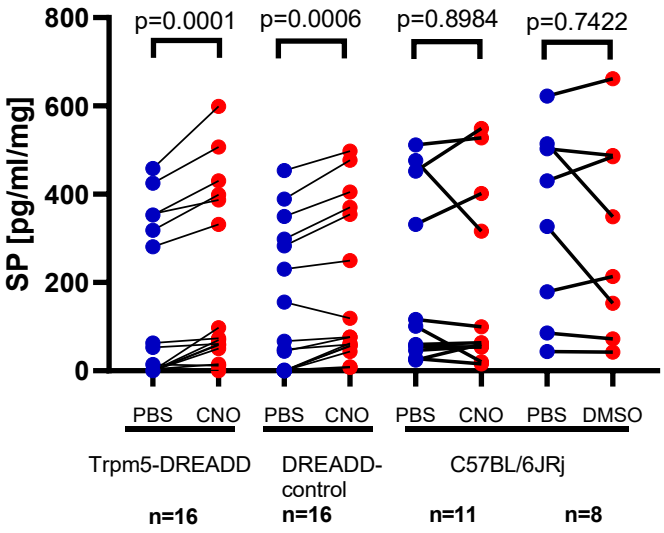

Figure 3.1: CNO induced neuropeptide release from *Trpm5*-DREADD and DREADD control, but not from C57BL/6JRj urethrae. ELISA to measure SP

concentration in the supernatants of explanted urethrae from T*rpm5*-DREADD, DREADD control and C57BL/6JRj mice after initial PBS administration and subsequent application of PBS with CNO (60 µM) for 10 min. Statistical analysis: Wilcoxon matched-pairs signed rank test.

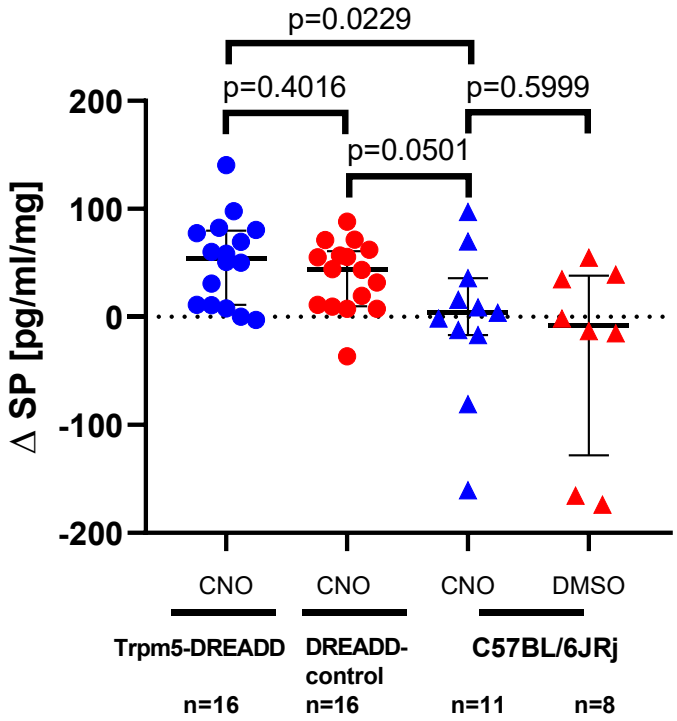

Figure 3.2: CNO induced neuropeptide release from *Trpm5*-DREADD and DREADD control, but not from C57BL/6JRj urethrae. SP release (calculated from data shown in Figure 3.1) from explanted urethrae in response to exposure to CNO (60 µM) in *Trpm5*-DREADD, DREADD control, and C57BL6/6JRj mice. Graph shows median and interquartile range. Statistical analysis: Mann-Whitney test, exact p values are indicated.

3.2 ChR2 is expressed in UTCs in *Chat-ChR2-EYFP* mice

In the optogenetic model, a fusion protein consisting of the blue light-activated cation channel ChR2 and EYFP is expressed under the control of the *Chat* promoter (*Chat*-ChR2-EYFP). When exposed to blue light, ChR2 opens, allowing sodium ions to enter the cell and causing depolarization (Zhao et al. 2011). We previously showed that ChR2-EYFP is selectively expressed in tuft cells in trachea and gall bladder in this mouse strain and that blue light from an LED source triggers mediator release from these tuft cells (Perniss et al. 2020; Keshavarz et al. 2022). It remained to be shown that ChR2-EYFP is also expressed by UTCs.

Results

DCLK1 is expressed in mouse tracheal and in human gallbladder tuft cells and it was used as a tuft cell marker in these organs (Montoro et al. 2018, Schutz et al. 2019). This has recently been also validated by our group for the mouse urethra (Schmidt et al., 2025). So, I applied DCLK1-antibody on the epithelium of *Chat-ChR2-EYFP* murine urethra to label UTCs, and gallbladder was used as a positive control. Cryosections from murine gallbladder immunolabeled with the antibody against DCLK1 showed flask-shaped immunoreactive cells with apical and basal processes (Figure 3.3A).

Urethral cryosections from *Chat-ChR2-EYFP* mice were immunolabeled with antibody against DCLK1. DCLK1-immunoreactive cells were observed in the urethral epithelium with apical and basal processes extending from the cell body. DCLK1-immunoreactivities were detected in the whole cell (Figure 3.3B and D). No immunolabeling was observed when the primary antibody was omitted (Figure 3.3E).

Colocalization of DCLK1-immunoreactivities and native EYFP-fluorescence was (44/50) 88%, which means that the vast majority of UTCs expresses ChR2 in this mouse strain (Figure 3.3B). On the other hand, single EYFP-positive cells accounted for 4% (Figure 3.3C), and single DCLK1-immunoreactive cells constituted 8% (Figure 3.3D). The percentages of colocalization are shown in the graph in Figure 3.4.

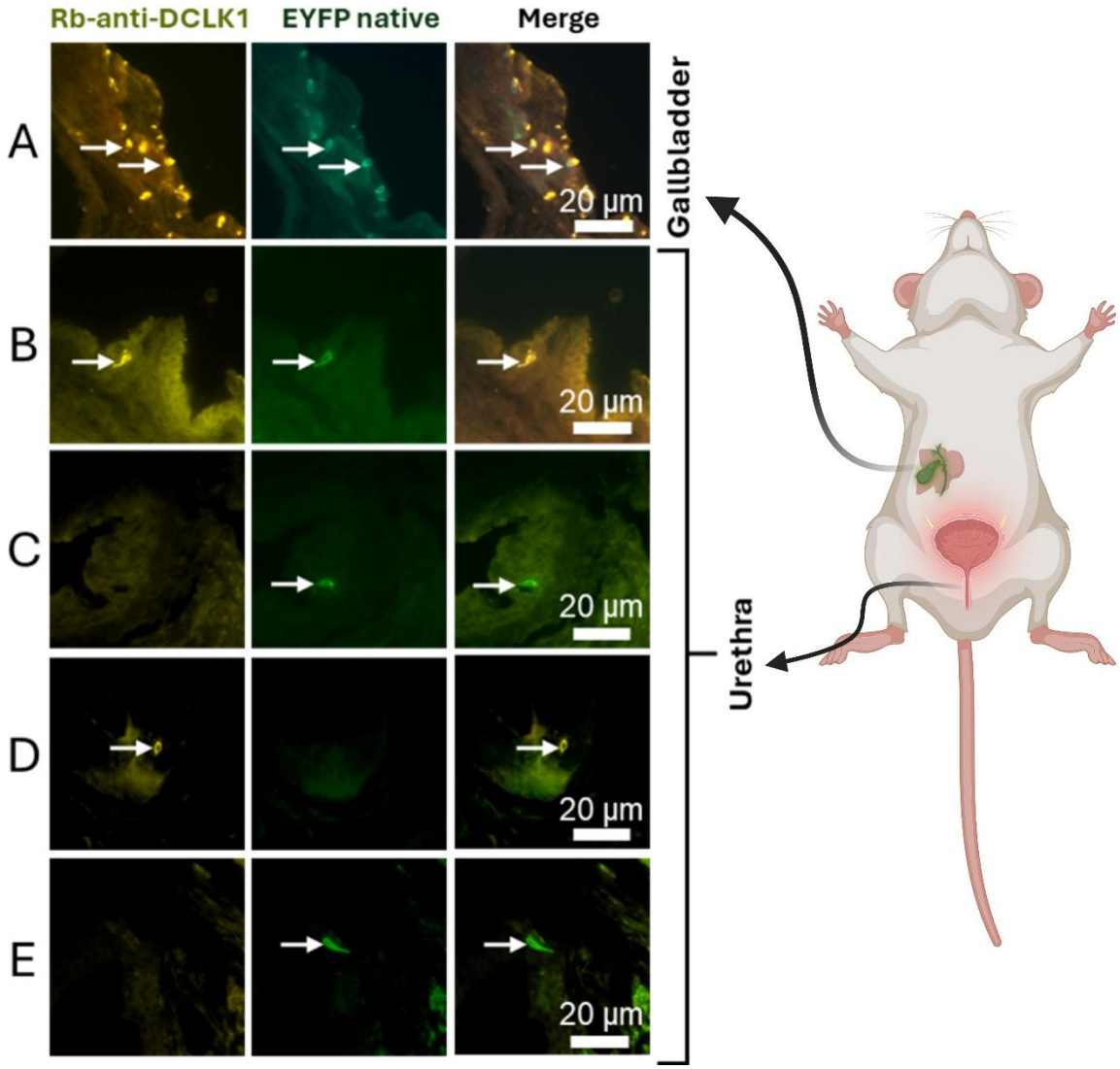

Figure 3.3: ChR2 is expressed in UTCs in *Chat-ChR2-EYFP* mice. ***(A)*** Immunohistochemistry of mouse gallbladder (positive control) cryosection from a *Chat-ChR2-EYFP* mouse, immunolabeled with antibody against DCLK1, showing cells double positive for DCLK1 and EYFP (arrows). Images captured with color camera; Image J was used to merge images. ***(B-D)*** Immunohistochemistry of urethral cryosections immunolabeled with antibody against DCLK1 showing epithelial cells (***B***) double positive for DCLK1 and EYFP (arrows), (***C***) single positive for native EYFP (arrows), ***(D)*** single positive for DCLK1 (arrows). ***(E)*** No immunoreactivity was observed when the primary antibody was omitted. Images were captured with black and white camera; Image J was used to color and merge images.

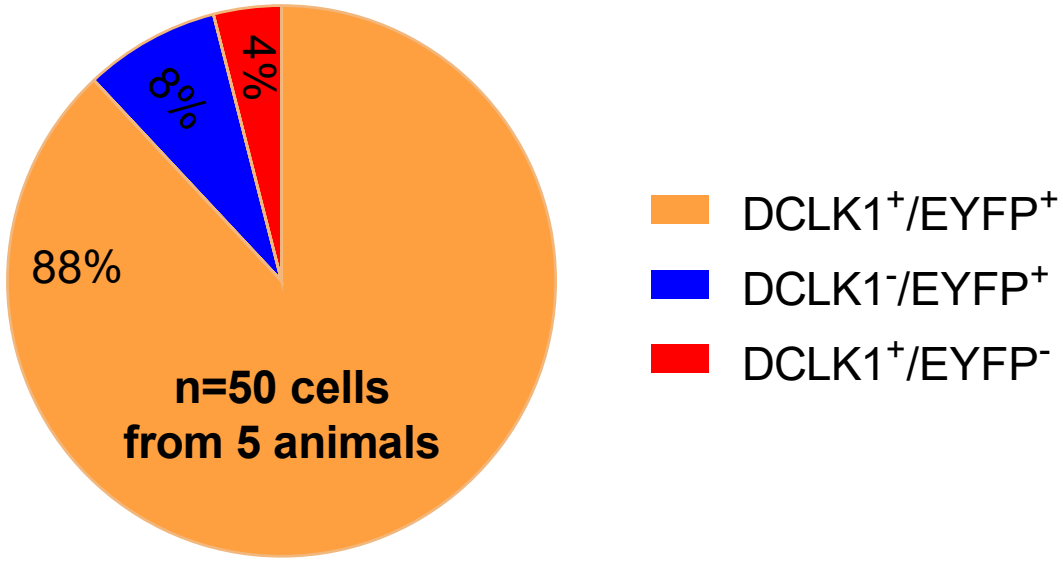

Figure 3.4: ChR2 is expressed in UTCs in *Chat-ChR2-EYFP* mice. Chart showing the percentage of phenotypes related to the total number of native EYFP fluorescent and DCLK1-immunolabeled cells in urethral cryosections from *Chat-ChR2-EYFP* mice. (15 sections, n=5 urethrae).

3.3 Sensory peptidergic fibers in the urethral mucosa do not express *Chat*-ChR2-EYFP

To see whether ChR2-EYFP expression is specific for UTC or might also occur in peptidergic nerve fibers, which would have impact on measurements of neuropeptide release, urethral cryosections from *Chat-ChR2-EYFP* mice were immunolabeled with antibodies against CGRP and SP. CGRP- and SP-immunoreactive nerve fibers were observed in the urethral epithelium. Sensory peptidergic fibers in the urethral mucosa did not express Chat-ChR2-EYFP (Figure 3.5A and B), excluding direct activation of nerve fibers by blue light in this mouse model.

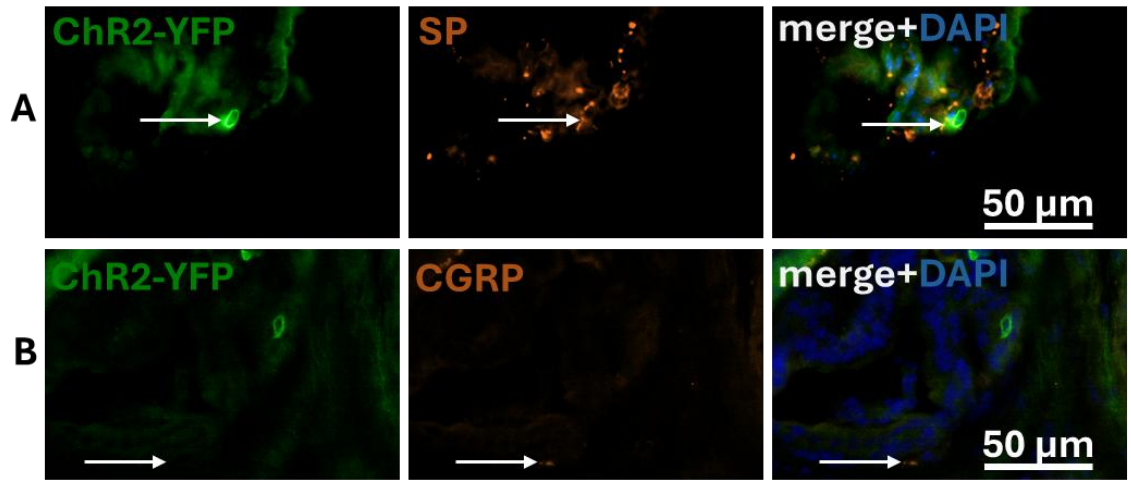

Figure 3.5: Peptidergic nerve fibers next to UTC are *Chat*-ChR2-EYFP negative. Urethral cryosection; native EYFP fluorescence and immunolabeling with antibodies against (***A***) SP or (***B***) CGRP in urethral mucosa of *Chat*-ChR2-EYFP mice. Small arrows: Peptidergic (SP or CGRP) but *Chat*-ChR2-EYFP negative fibers near to *Chat*-ChR2-EYFP positive UTC.

3.4 Stimulation of urethrae from *Chat*-ChR2-EYFP-mice with LED blue light induced release of SP

Using the methodology described in chapter 3.1, the exposure of explanted urethrae from *Chat*-ChR2-EYFP-mice to blue LED light yielded the following.

In *Chat*-ChR2-EYFP transgenic mice, the SP content in supernatants taken after LED illumination was significantly higher than that in the first supernatant ($p=0.0134$; Wilcoxon matched-pairs signed rank test) with an median SP release (defined as difference in the concentrations of the two supernatants) of 7.76 pg/ml per mg of urethra. In corresponding control mice, supernatants of explanted urethra after exposure to LED blue light showed an median SP release of -3.60 pg/ml per mg of urethra with no significant difference between supernatants taken before and after LED exposure ($p=0.2036$; Wilcoxon matched-pairs signed rank test) (Figure 3.6).

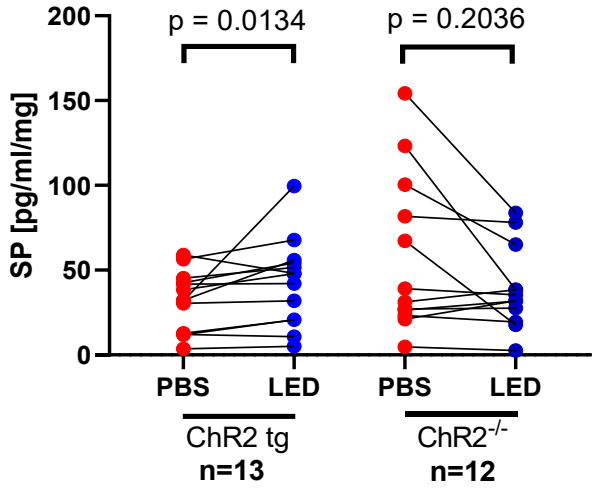

Figure 3.6: Stimulation of urethrae from *Chat*-ChR2-EYFP-mice with LED blue light induces release of SP. ELISA, SP concentration in the supernatant of explanted urethrae from *Chat*-ChR2-EYFP transgenic mice (Chr2 tg) and control mice (ChR2$^{-/-}$) after initial PBS administration and subsequent exposure to LED blue light for 10 min. Statistical analysis: Wilcoxon matched-pairs signed rank test, exact p values are indicated.

Comparing both strains, the release of SP from urethrae of *Chat*-ChR2-EYFP transgenic mice induced by LED blue light administration was significantly higher than the Δ-values seen in controls (p=0.0045; Mann-Whitney test) (Figure 3.7).

These results demonstrate that optogenetic activation of ChAT-expressing UTC via blue light stimulation specifically induces significant SP release in the urethra of *Chat*-ChR2-EYFP transgenic mice.

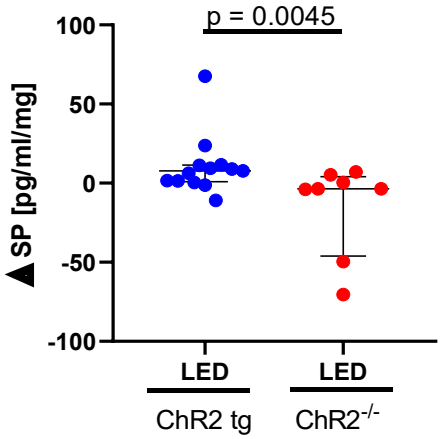

Figure 3.7: Stimulation of urethrae from *Chat*-ChR2-EYFP-mice with LED blue light induces release of SP. ELISA, SP release (calculated from data shown in Figure 3.6) from explanted urethrae in response to exposure to LED blue light for 10 min.

ChR2 tg: *Chat*-ChR2-EYFP transgenic mice, ChR2$^{-/-}$ control mice of both sexes. Graph shows median and interquartile range. Statistical analysis: Mann-Whitney test, exact p values are indicated.

3.5 Optogenetically induced SP release is fully blocked by the general nicotinic receptor blocker mecamylamine

The data so far indicated that activation of UTC leads to neuropeptide (SP) release from nearby nerve fibers, implying communication between UTC and sensory terminals. All hitherto known examples of UTC-to-neuron communication rely on cholinergic signaling with UTC-derived acetylcholine acting upon acetylcholine receptors on sensory nerve fibers (Billipp et al., 2024). Our group previously showed that UTC are in contact with sensory nerve fibers expressing a nicotinic acetylcholine receptor, and a nicotinic receptor blocker inhibited reflex detrusor muscle activation upon intraurethral application of the bitter substance, denatonium (Deckmann et al., 2014). Thus, we tested whether SP release from sensory nerve terminals upon optogenetic stimulation of UTC is also triggered by cholinergic communication involving nicotinic receptors.

Urethrae from *Chat*-ChR2-EYFP transgenic were incubated for 10 min in PBS as before and then exposed to blue LED light for another 10 min in PBS in the absence or presence of mecamylamine (20 µM), a general nicotinic receptor inhibitor.

Confirming the results from the previous experimental series (chapter 3.4), exposure to LED blue light without addition of a blocker caused a significant increase in SP content in the supernatant of urethrae explanted from *Chat*-ChR2-EYFP transgenic mice ($p=0.0322$; Wilcoxon matched-pairs signed rank test). This was not the case, however, when mecamylamine (20 µM) was added ($p=0.0840$; Wilcoxon matched-pairs signed rank test) (Figure 3.8).

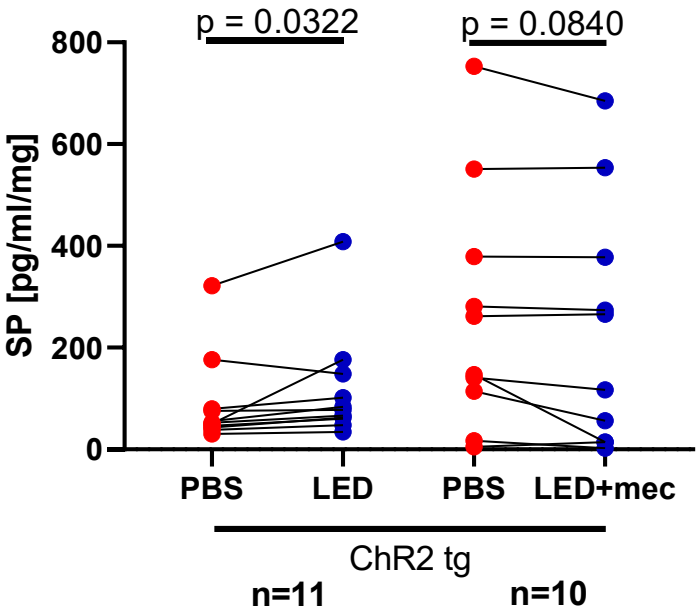

Figure 3.8: Optogenetically induced SP release is fully blocked by the general nicotinic receptor blocker mecamylamine. ELISA, SP concentration in the supernatant of explanted urethrae from *Chat*-ChR2-EYFP transgenic mice after initial PBS administration and subsequent exposure to LED blue light for 10 min in the absence or presence of the nicotinic receptor blocker, mecamylamine (20 µM). Statistical analysis: Wilcoxon matched-pairs signed rank test.

Without mecamylamine, SP release amounted for 13.84 pg/ml/mg (median), whereas the median difference in SP content between supernatants taken before and after LED illumination in the presence of mecamlyamine (20 µM) was -10 pg/ml/mg. The difference in SP release between both groups was statistically significant (p=0.0011; Mann-Whitney test) (Figure 3.9).

These findings show that activation of nicotinic acetylcholine receptors is necessary for the communication between UTCs and nearby sensory neurons triggering SP release.

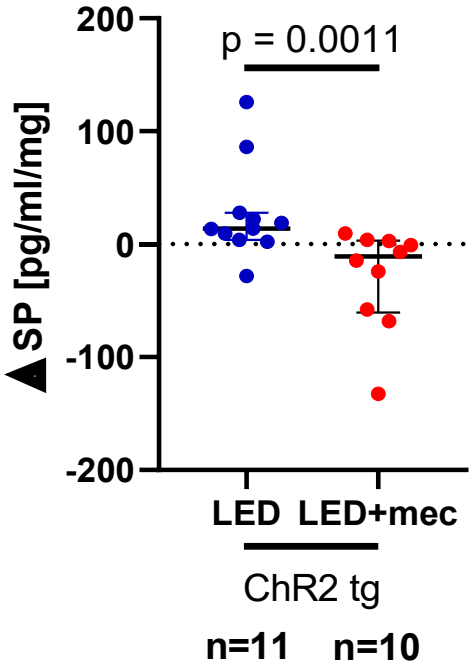

Figure 3.9 Optogenetically induced SP release is fully blocked by the general nicotinic receptor blocker mecamylamine. ELISA, SP release (calculated from data shown in Figure 3.8) from explanted urethrae of *Chat*-ChR2-EYFP transgenic mice (ChR2 tg) in response to exposure to LED blue light for 10 min in the absence or presence of the nicotinic receptor blocker, mecamylamine (20 µM). Graph shows median and interquartile range. Statistical analysis: Mann-Whitney test.

3.6 Denatonium triggers UTC-dependent SP release from explanted urethrae

The data so far showed that experimentally induced depolarization of UTC can initiate cholinergic nicotinic signaling to sensory neurons with the consequence of SP release. As a next step, it was investigated whether such an effect can also be triggered by chemical stimulation of receptors endogenously expressed by UTC. The stimulus to be tested was denatonium, a bitter tasting substance that activates tuft cells of various organs and is known to induce rise in intracellular calcium concentration in UTC (Deckmann et al. 2014; Deckmann et al. 2018). Since denatonium might also activate other cell types in addition to UTC, urethrae from a mouse strain that lacks UTC due to genetic deficiency of the transcription factor Pou2f3 (*Pou2f3*$^{-/-}$ mice) were included in this study.

Results

In *Pou2f3*$^{+/+}$ mice, denatonium (5 mM) evoked a significant release of SP from explanted urethrae (p=0.0039; Wilcoxon matched-pairs signed rank test) with a median of 70.55 pg/ml/mg of urethra. In *Pou2f3*$^{-/-}$ mice, lacking UTC, supernatants of explanted urethra after incubation with denatonium showed no significant release of SP (p=0.1250; Wilcoxon matched-pairs signed rank test) (Figure 3.10). The median difference in SP content between supernatants from *Pou2f3*$^{-/-}$ urethrae taken before and after denatonium was significantly smaller (3.75 pg/ml/mg) than that evoked in *Pou2f3*$^{+/+}$ mice (71 pg/ml/mg, p=0.022 Mann-Whitney test) (Figure 3.11).

Capsaicin (1 mM), serving as an UTC-independent direct activator of peptidergic sensory nerve terminals, evoked a significant SP release from explanted urethrae of *Pou2f3*$^{+/+}$ mice (p=0.0078; Wilcoxon matched-pairs signed rank test) and *Pou2f3*$^{-/-}$ mice (p=0.0078; Wilcoxon matched-pairs signed rank test) (Figure 3.10) to equal extent in both mouse strains (p=0.7984; Mann-Whitney test) (Figure 3.11).

These findings indicate that while denatonium-induced SP release from the explanted urethra is largely dependent on UTCs and significantly reduced in their absence, capsaicin can elicit comparable SP release independently of UTCs.

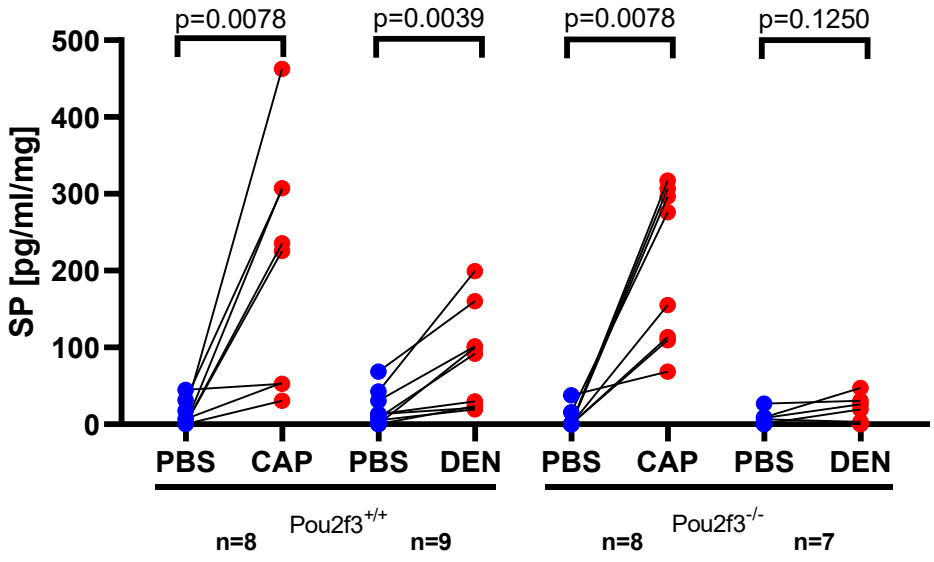

Figure 3.10: Denatonium triggers UTC-dependent SP release from explanted urethrae. ELISA, SP concentration in the supernatant of explanted urethrae from *Pou2f3*$^{+/+}$ and *Pou2f3*$^{-/-}$ mice after initial PBS administration and subsequent application of denatonium (5 mM) or capsaicin (1 mM) as a positive control. Statistical analysis: Wilcoxon matched-pairs signed rank test.

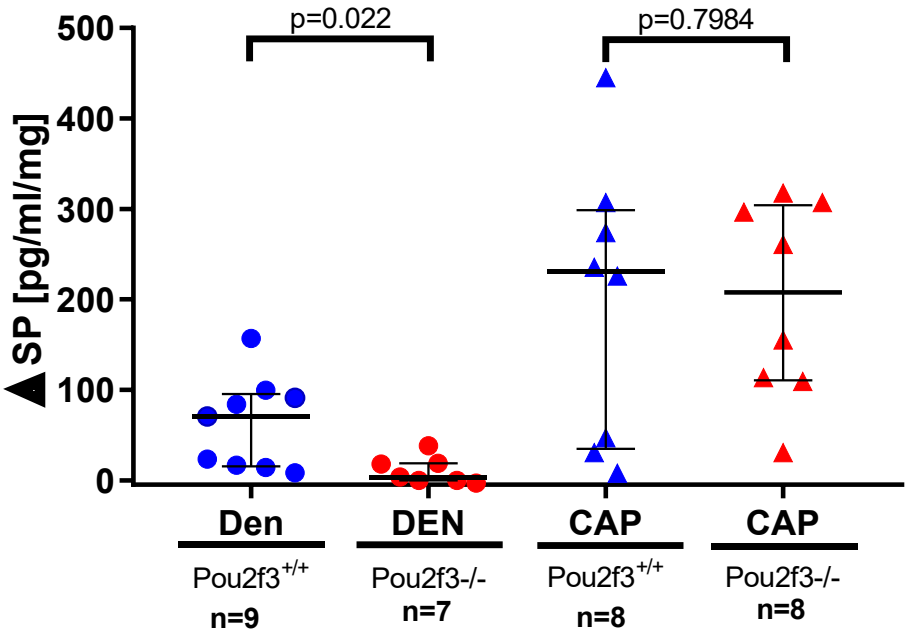

Figure 3.11: Denatonium triggers UTC-dependent SP release from explanted urethrae. ELISA, SP release (calculated from data shown in Figure 3.10) from explanted urethrae of *Pou2f3*$^{+/+}$ and *Pou2f3*$^{-/-}$ mice of both sexes in response to incubation for 10 min with 5 mM denatonium or 1 mM capsaicin. Graph shows median and interquartile range. Statistical analysis: Mann-Whitney test.

4 Discussion

4.1 (Un)suitability of the DREADD model to study cholinergic effects driven by UTC

In this study, we tested if the activation of UTCs could cause release of the neuropeptide SP from adjacent (nearby) peptidergic sensory nerve terminals. Since still no selective chemical stimulus of UTC is known, we tested genetic mouse models for their suitability to selectively stimulate UTC without activating other cells. One potential model was based on DREADD expression. DREADD is the abbreviation of “designer receptors exclusively activated by designer drugs”, genetically engineered G protein–coupled receptors (GPCRs) derived from human muscarinic acetylcholine receptors. These receptors have been mutated so that they no longer respond to their endogenous ligand, i.e. acetylcholine. Instead, they are selectively activated by a synthetic ligand, in this case CNO, which at the end causes increase in intracellular Ca^{2+} concentration (Armbruster et al. 2007; Roth 2016). The mouse strain used in this study expresses DREADD under the control of the *Trmp5* promotor (Qiao et al., 2023), which shall confer specificity to UTC. Indeed, our group showed by several techniques including the use of *Trpm5*-reporter mice, that UTC are the only cell type in the mouse urethra, which expresses *Trpm5*. Particular care was taken to exclude *Trmp5* expression by sensory neurons, which would have led to direct neuropeptide release without prior UTC activation (Schmidt et al. 2025). Still, CNO application induced a robust release of SP in both *Trpm5*-DREADD and DREADD control mice.

We hypothesized that, the release of SP from DREADD control could be due 1) to CNO acting on another receptor, or 2) to some *Trpm5*-independent expression (“leaky” expression) of the DREADD in mice carrying the DREADD construct in their genome but not set under control of the *Trpm5* promotor (DREADD control mice). In support of possibility #1, previous studies showed that CNO itself does not activate other receptors, but is metabolized to clozapine, which can act on endogenous receptors such as dopamine (D_2, D_4), serotonin (5-HT_2A, 5-HT_2C), muscarinic acetylcholine (M_1–M_5), adrenergic (α_1, α_2), and histamine (H_1) receptors (Gomez et al., 2017). If this were the reason for CNO-induced SP release, the same effect shall occur in wild-type mice, which do not carry the DREADD gene in their genome at all. Therefore, I tested CNO on urethrae of wild-type C57BL/6JRj mice. In these experiments, no SP release was observed. The absence of an effect in urethrae from C57BL/6JRj mice shows that CNO

itself does not directly stimulate SP release in the absence of the transgene, supporting its specificity in principle. Rather, “leaky” expression of DREADD in the control mouse model is currently considered the most likely explanation. Although this could have been further examined using immunolabeling or PCR, such experiments were not conducted, as their outcomes would not have clarified the underlying question, i.e. whether activation of UTC triggers neuropeptide release from sensory nerve fibers.

Nonetheless, even if there were “leaky” expression of DREADD is some cells in the control, one might expect a higher release of SP in DREADD mice, which, in addition, show *Trpm5*-driven DREADD expression in UTC. This, however, was not the case, indicating that either, against expectation, DREADD is not sufficiently expressed in UTC, or the intracellular signaling pathway following DREADD activation is not linked to acetylcholine release from UTC, which is responsible for triggering SP release from nerve endings. Although, as explained above, no further attempts were undertaken to clarify the reason underlying the unsuitability of the model, there is evidence in favor of non-linked intracellular pathways. Failure to induce cholinergic effects driven by tuft cell chemogenetic models has also been reported for the small intestine (Bilipp et al., 2024). These authors used two different mouse lines to achieve DREADD expression in intestinal tuft cells. Both are based, like the one I used, on expression of Cre recombinase driven by a tuft cell-specific promotor, which then cuts out the floxed STOP signal in the DREADD constrict, thereby activating its expression. The authors used constitutive (*Il25*-Cre) - interleukin-25 is specifically expressed in intestinal tuft cells (Gerbe et al., 2016; von Moltke et al., 2016; Howitt et al., 2016) - and inducible (Pou2f3$^{Cre\text{-}ERT2/+}$) Cre to drive tuft cell-specific expression of Gq- or Gi-coupled DREADDs and confirmed the expression of hemagglutinin-tagged DREADDs in tuft cells. Yet, stimulation with their synthetic ligand (compound 21, a synonym for CNO) failed to elicit fluid secretion in the proximal or distal small intestine. The authors reasoned that this may indicate that the G proteins necessary for DREADD signaling are absent in tuft cells, or that the downstream signals generated upon DREADD activation are insufficient to trigger acetylcholine release (Billipp et al. 2024).

While the present data show that the chemogenetic model was not suitable to evoke an effect that is based upon acetylcholine release from UTC, a recent report using the same mouse line demonstrated ATP release from tracheal tuft cells upon stimulation with CNO (Abdel Wadood et al., 2025), supporting the notion that DREADD is

expressed in tuft cells in this mouse strain. The positive outcome in this study may indicate that different intracellular pathways in tuft cells govern ATP and acetylcholine release.

Taken together, these results emphasize the need for alternative strategies to study UTC-nerve interactions in the urethra, and the suitability of an optogenetic model was explored.

4.2 Selective expression of ChR2 in UTC in the optogenetic model

In search of a model allowing selective activation of UTC, we turned to the *Chat*-ChR2-EYFP mouse (B6.Cg-Tg(Chat-COP4*H134R/EYFP,Slc18a3)6Gfng/J; (Zhao et al., 2011), a transgenic model in which the light sensitive cation channel ChR2 is expressed under control of the *Chat* promoter. When exposed to blue light (~470 nm), ChR2 opens and allows the rapid influx of cations across the plasma membrane, producing membrane depolarization. Channelrhodopsins are not naturally occurring in mammals, but in algae. They make these organisms sensitive to visible light, enabling them to move towards the light (phototaxis) to maintain efficient photosynthesis (Nagel et al., 2003). Targeted, cell type-specific expression of ChRs in model organisms such as *Caenorhabditis elegans* and mice has been introduced as an experimental tool allowing cell type-specific depolarization, mainly used in neuroscience (Boyden et al., 2005). Several variants (mostly point mutations) of the original sequence have been generated, which differ in channel conductance, kinetics, desensitization, light sensitivity, spectral response, membrane trafficking and expression (Lin 2011). The variant used in the present study, ChR2/H134R, is characterized by increased photocurrents, which shall enhance cell activation, but slower kinetics than the wildtype ChR2 (Lin 2011). While slower kinetics may be of disadvantage in neuroscience experiments requiring high temporal resolution, they are irrelevant in the context of the present study in which the readout (collection of supernatants for analysis of SP content) is done after 10 min of stimulation.

In this model, other than in the chemogenetic model that utilizes the *Trpm5* promotor, expression of the transgene is driven by the *Chat* promotor. *Per se*, this does not necessarily confer cell specificity to UTC, because there are several other cell types that produce acetylcholine, which is synthesized by ChAT. The most prominent example are postganglionic parasympathetic neurons using acetylcholine as their primary neurotransmitter, but also several non-neuronal cells, in particular cells of the

immune system, utilize acetylcholine as a messenger molecule (Wessler et al., 1998; Kummer and Krasteva-Christ 2014; Dai 2025). Theoretically, genetic models relying on the activity of the *Chat* promotor can be expected to drive expression in all these cell types. In practice, however, the various mouse strains generated so far can differ markedly in cell specificity, and there are even regional differences. For example, an often used *Chat*-EGFP (enhanced green fluorescent protein) reporter mouse strain (B6.Cg-Tg(RP23-268L19-EGFP)2Mik/J; Tallini et al., 2007) lacks visible EGFP in most cholinergic parasympathetic neurons of the heart and airways, whereas it fully delineates cholinergic neurons in the bladder and intestines (Brown et al., 2018). In the brain of these mice, there is complete overlap between the transgenic expression of EGFP and immunohistochemical staining for ChAT in the areas of the cholinergic basal forebrain, whereas cholinergic cells of the tegmental nuclei lack EGFP expression (Gamage et al., 2023). While this mouse line shows strong expression of the transgene in tuft cells of all locations including the gallbladder (Krasteva et al., 2011; Deckmann et al., 2014; Keshavarz et al., 2022), tuft cells of the gallbladder (other locations not tested) remain unlabeled in a mouse strain expressing a fusion protein of the red fluorescent protein tdTomato and ChR2 in a model based on *Chat*-driven Cre expression (Keshavarz et al., 2022). Therefore, the expression pattern of the transgene needs to be carefully evaluated for each organ and tested for its suitability in the context of the aim of the study.

On this background, a mouse line (B6.Cg-Tg(Chat-COP4*H134R/EYFP,Slc18a3)6Gfng/J; Zhao et al., 2011) was chosen for the present study, which our group previously had used successfully for studying tracheal and gallbladder tuft cell function (Perniss et al., 2020; Keshavarz et al., 2022). First, we aimed to answer the question: is ChR2 truly expressed in UTCs of these mice? Immunohistochemical analysis using an antibody against DCLK1, a well-established tuft cell marker across multiple organs (Saqui-Salces et al., 2011; Middelhoff et al., 2017) revealed a striking overlap (88%) between DCLK1-immunoreactivity and native EYFP fluorescence in the urethral epithelium. Similar ChR2-EYFP expression patterns have been reported in the trachea and gallbladder, where tuft cells respond to optical stimulation by releasing signaling mediators (Perniss et al., 2020; Keshavarz et al., 2022). Notably, visible EYFP fluorescence directly indicates the position of the ChR2 protein in this model, since they are expressed as a fusion protein. These findings indicate that UTC of these mice shall be susceptible to light-activated depolarization.

With the expression of ChR2 in UTCs established, we investigated whether ChR2 is also expressed in other cellular elements of the urethra. Although sensory neurons are mostly not considered to be cholinergic, expression of an mRNA splicing variant of *Chat* lacking exons 6 to 9 has been reported in sensory neurons, the resulting protein being called pChAT (peripheral type of ChAT) (Tooyama and Kimura 2000; Yasuhara et al., 2007; Bellier and Kimura 2007). There is dispute about the actual capacity of pChAT to synthesize relevant amounts of acetylcholine because of the lack of His^{334} (histidine residue at position 334 of the amino acid sequence) acting as the catalytic center (Bellier and Kimura 2011). Nonetheless, select subpopulations of sensory neurons show up in some *Chat* reporter mouse strains, and this includes a few peptidergic (SP^+/$CGRP^+$) neurons in sacral dorsal root ganglia that provide sensory innervation to the lower urinary tract (Schmidt et al., 2025). Therefore, particular attention was paid to ChR2-EYFP expression by sensory neurons, because then optical stimulation could directly excite nerve fibers, masking a potential contribution of tuft cells. To investigate this, we analyzed the distribution of peptidergic nerve fibers within the urethral mucosa using immunostaining for SP and CGRP. This revealed peptidergic fibers coursing just beneath the epithelial surface, closely to ChR2-EYFP-positive UTC, but none of the SP- or CGRP-positive fibers exhibited ChR2-EYFP fluorescence.

These findings provided evidence that ChR2 expression in the urethra of *Chat*-ChR2-EYFP mice is restricted to UTC and absent from sensory peptidergic neurons, providing a basis for selective stimulation of UTC by blue light.

4.3 Optogenetic activation of UTCs links to acetylcholine release

We next asked a key question: can blue LED light induce release of acetylcholine from ChR2-expressing tuft cells?

When urethrae from *Chat*-ChR2-EYFP mice were illuminated with blue LED light, we detected an increase in SP release, a neuropeptide produced by sensory neurons, which was prevented by the nAChR inhibitor, mecamylamine. Control tissues, identical in preparation but lacking ChR2 expression, remained unresponsive under the same conditions. Thus, optogenetic stimulation triggered a cholinergic effect, indicating acetylcholine release from UTC. In principle, blue LED light activation of ChR2 in cells depolarizes their membranes through cation influx, which triggers intracellular signaling pathways and the release of neurotransmitters such as acetylcholine or

glutamate from neurons (Coli et al., 2024). Although not explicitly analyzed, it is assumed that the ChR2 variant used in this study, ChR2/H134R, shows the same ion permeability as ChR2, i.e. being non-selectively permeant towards H^+, Na^+, K^+ and Ca^{2+} (Lin 2011). Under physiological conditions, Na^+ influx dominates and is the main determinant of membrane depolarization. This optogenetically induced depolarization mimics physiological excitation, leading to opening of voltage-dependent Ca^{2+}-channels, increase in intracellular Ca^{2+}-concentration, which then leads to exocytotic release of neurotransmitters from their storage vesicles in neurons (Coli et al., 2024). As a prerequisite, neurotransmitters have first to be enriched in synaptic vesicles. In case of acetylcholine, synthesis happens via ChAT in the axoplasm and acetylcholine is then translocated into the interior of synaptic vesicles via the vesicular acetylcholine transporter (VAChT).

While this is the canonical way of acetylcholine synthesis and release from neurons, there are alternative pathways in many non-neuronal cells, including tuft cells (Kummer et al., 2008; Pan et al., 2020; Dai 2025). Specifically, absence of VAChT expression has been reported (Schütz et al., 2015) and direct release of acetylcholine from the cytoplasm through the plasma membrane into the surrounding is assumed (Dai 2025). Indeed, several membrane transporters have been identified that are permeable for acetylcholine and can confer its release from cells. These include organic cation transporters 1-3 (OCT1-3; Wessler et al., 2001; Lips et al., 2005), organic cation transporter novel member 1 (OCTN1; Pochini et al., 2012; Pochini et al., 2024), choline transporter-like protein 4 (CTL4; Song et al., 2013), mediatophore, a homooligomer of a 16-kDa subunit homologous to the proteolipid subunit c of vacuolar H^+-ATPase (Israël et al., 1988; Fujii et al., 2012), and release through hemichannels is also assumed (Dai 2025). Little is known, however, if and how acetylcholine release through these transmembrane mechanisms is regulated. OCTN1 has an intracellular ATP-binding cassette promoting transport (Pochini et al., 2012), whereas acetylcholine transport via OCTs is passive, bidirectional, and depends on concentration gradient and, because of the positive charge of acetylcholine, on membrane potential (Lips et al., 2005). Hence, cation influx resulting from opening of ChR2 may facilitate acetylcholine efflux, but whether this is truly the link from ChR2 activation to acetylcholine release from UTC warrants further experimental proof.

It also needs to be considered that acetylcholine release from UTC in the genetically modified *Chat*-ChR2-EYFP mice may differ from that in wildtype animals. In this strain, cholinergic specificity is ensured by using bacterial artificial chromosome (BAC) transgenic mice expressing a ChR2-EYFP fusion protein under the control of the *Chat* promoter (Zhao et al., 2011). Importantly, the BAC containing the *Chat* gene carries also the *Vacht* gene. Both proteins are encoded by the so-called “cholinergic gene locus”, where the entire, intron-less coding sequence of *Vacht* lies in the first intron of the non-coding sequence of the *Chat* gene (Bejanin et al., 1994; Erickson et al., 1994; Roghani et al., 1994). Hence, these mice carry multiple copies of the *Vacht* gene and, at least in the brain, overexpress functional VAChT with functional consequences. They present enhanced motor endurance but show deficits in attention and several additional cognitive domains (Kolisnyk et al., 2013). It remains to be determined whether *Vacht* is overexpressed also in UTC of these mice and whether this may alter release dynamics of acetylcholine, potentially even shifting from non-vesicular to vesicular release.

4.4 Nicotinic signaling from UTCs to sensory fibers

After establishing that optogenetic activation of UTCs induces the release of acetylcholine from UTCs and subsequent release of SP, we next wanted to know what molecular mechanism(s) drive(s) this epithelial-neuronal communication. The questions arose: Is acetylcholine the primary and only neurotransmitter that links tuft cell to sensory neurons, and which receptor class is involved?

To answer this question, we first tested if nAChR antagonism alters the SP response. In control conditions, illumination of *Chat*-ChR2-EYFP–positive UTCs with blue LED light induced SP release as previously described. However, when we applied mecamylamine, a broad-spectrum nicotinic receptor blocker, the SP response was completely stopped, indicating that, under these conditions, acetylcholine is the sole transmitter and acts on nAChR on peptidergic sensory nerve terminals.

This finding aligns with earlier evidence that acetylcholine serves as the primary signaling molecule in tuft cell-to-neuron interactions. Tuft cell-derived acetylcholine acting on sensory nerve fibers can trigger long-distance reflexes and local neurogenic inflammation, and nAChR are involved in both cases. In the trachea, respiratory depression upon exposure to the bitter tastant cycloheximide, a product of the Gram-positive bacterium *Streptomyces griseus*, is fully prevented by mecamylamine

(Krasteva et al., 2011). In the nose, blocking nicotinic, but not muscarinic, acetylcholine receptors prevents neurogenic inflammation mediated through SCC for both denatonium and the bacterial signaling molecule 3-oxo-C12-homoserine lactone (Saunders et al., 2014). In the urethra, however, Deckmann et al. (2014) reported that nAChR blockade by mecamylamine instilled into the urethral lumen largely reduces, but not abolishes denatonium-induced bladder reflexes. Further, in a follow-up study of the present work, denatonium-induced SP release from explanted urethrae was also only reduced but not completely abrogated by mecamylamine (Schmidt et al. 2025). The nature of the mecamylamine-resistant component remained unsolved. In the reflex study, it had been discussed that mecamylamine might not have crossed the tight urothelium in a concentration high enough to block transmission between UTC and sensory fibers (Deckmann et al., 2014). This, however, can merely explain the mecamylamine-resistant component in the SP release experiments conducted on explanted urethrae, in which mecamylamine has direct access to the deeper tissue layers. It also had been discussed that co-release of other neuroactive substances, such as ATP, might act in parallel (Deckmann et al., 2014). Indeed, tuft cells at other locations can release, in addition to acetylcholine, cysteinyl-leukotrienes (gallbladder: Keshavarz et al. 2022; airways: Perniss et al., 2020; Bankova et al., 2018; intestine: McGinty et al., 2020; Pan et al., 2020) and ATP (trachea: Abdel Wadoud et al., 2025), which both can activate populations of sensory nerve fibers (Andersson 2002; Burnstock 2000; Kinnamon and Finger 2022; Voisin et al., 2021). If this were the reason for the mecamylamine-resistant component in the denatonium experiments, then it shall be assumed that denatonium and optogenetic stimulation induce a different profile of mediator release, because a mecamylamine-resistant component was not seen in the optogenetic model. Cysteinyl-leukotrienes are not the prime candidates for making this difference, since, at least in the gallbladder, they are released together with acetylcholine from tuft cells upon optogenetic activation of tuft cells in this mouse strain (Keshavarz et al., 2022). On the other hand, it also shall be noted, that plasma extravasation induced by denatonium acting on SCC in the nose was fully sensitive to mecamylamine (Saunders et al., 2014), mimicking that what we found in the present study for optogenetically induced SP release in the urethra.

While the mechanisms underlying the mecamylamine-resistant effects in certain experimental setups – e.g co-release of other mediators of unspecific effects of denatonium - remain to be clarified, the present study provides direct functional proof

that acetylcholine released from optogenetically stimulated UTCs activates nicotinic receptors on nearby peptidergic sensory to trigger SP release. It, thus, extends the concept of tuft cell-driven neuropeptide release through nicotinic signaling from the airways to the urethral epithelium. This highlights acetylcholine as a key mediator in the UTC network and highlights the *Chat*-ChR2-EYFP model as a strong model for studying cholinergic control of neuropeptide signaling in epithelial tissues.

4.5 Denatonium Induces UTC-dependent SP release in ex vivo urethrae

The present findings demonstrate that the bitter tastant denatonium evokes significant SP release from the urethra, and that this effect critically depends on the presence of UTCs when using denatonium at a concentration of 5 mM. In wild-type mice, denatonium exposure led to robust SP release, whereas in *Pou2f3*-deficient mice, which lack UTCs, this response was absent. These results are in full accordance with the data obtained in the optogenetic model and provide strong evidence that UTCs serve as the primary chemosensory cells responsible for initiating bitter compound induced epithelial neuronal signaling in the urethra.

This is consistent with earlier studies showing that tuft cells in multiple organs, including nose, trachea, and urethra, detect bitter substances, likely via taste receptors, and respond with intracellular calcium signaling and transmitter release (Tizzano et al., 2010; Krasteva et al., 2011; Deckmann et al., 2014; Deckmann et al., 2018; Abdel Wadood et at., 2025). Our data now extend this concept by directly linking bitter compound stimulation of UTCs to functional neuropeptide release from nearby sensory nerve terminals, underscoring the role of UTCs as pivotal epithelial sentinels.

Importantly, the specificity of the denatonium effect was verified using capsaicin as a control stimulus. Capsaicin, a direct activator of TRPV1-expressing sensory fibers, induced SP release to a similar extent in both wild-type and *Pou2f3*-deficient mice. This confirms that the lack of denatonium-induced SP release in *Pou2f3*$^{-/-}$ mice cannot be attributed to general defects in peptidergic signaling or nerve function but is specifically due to the absence of UTCs.

The requirement of UTCs for denatonium-evoked SP release highlights their critical role in translating luminal chemical cues into neuronal activation. This cholinergic–peptidergic signaling cascade may represent a protective pathway by which bitter-

tasting, potentially harmful compounds in the urethral lumen are detected and relayed to the nervous system. Through SP release, this pathway could contribute to neurogenic inflammation, heightened sensory signaling, and reflex control of the lower urinary tract, ultimately serving as an early-warning mechanism against noxious substances or pathogens.

In summary, the current results establish that **denatonium-induced SP release is a UTC-dependent process,** whereas direct nerve activation by capsaicin bypasses UTCs. This distinction reinforces the role of UTCs as specialized chemosensory intermediaries and provides further mechanistic insight into epithelial–neuronal communication in the urethral mucosa.

4.6 Downstream of SP release: neurogenic inflammation

Throughout all organs investigated so far, SP released from sensory nerve terminals, often together with CGRP, causes a neurogenic inflammation, which starts with plasma extravasation guided by SP acting on NK1 receptors on the endothelium of postcapillary venules and vasodilation mediated by CGRP acting CGRP receptors on the muscle (Holzer 1998). These downstream effects were not directly investigated in the present study, but there is evidence from previous work that this principle also applies to the urethra. In the urethra, plasma extravasation is caused by mechanical irritation like catheterization (Abelli et al. 1991), exposure to SP or capsaicin, a TRPV1 agonist typical of nociceptors, and antidromic electrical stimulation (Lundberg et al. 1984; Maggi et al., 1987; Pintér and Szolcsányi 1988).

So, the response is not limited to UTC activity. UTCs act as a mediator that enlarges the range of stimuli, which are able to trigger it.

UTC- and capsaicin-triggered responses are similar, but they may not rely on the same nerve fibers. At least for neurogenic inflammation induced by catheterization (mechanical irritation), it is clear that more than one peptidergic fiber type is involved, because desensitization of capsaicin-sensitive fibers by systemic pretreatment with capsaicin reduced neurogenic inflammation only by 50 % (Abelli et al., 1991). This indicates that the peptidergic fibers related to UTCs may also have diverse phenotypes. Accordingly, it remains unknown so far what the reflex responses of stimulation of the UTC-associated peptidergic fibers might be. As for the capsaicin-sensitive fibers in the urethra, it is known that their stimulation initially increases bladder

contractions (Lundberg et al. 1984; Maggi et al., 1987), which is consistent with a protective function in that it might flush out hazardous material. Since capsaicin soon causes desensitization of responsive nerve fibers, this bladder activing effect turns into a suppression after 15-30 minutes (Lundberg et al. 1984; Maggi et al., 1987), but this shall not be expected in response to natural stimuli.

There are at least two consequences resulting from plasma extravasation. The first one, soluble factors of the immune system circulating in the blood stream enter the tissue and might act as primary line of defense (Shishido et al., 2012, Hollenhorst et al., 2022). The second one, edema causes local swelling, which has a defense role as a result of mechanical effects; this has been found in the vomeronasal duct opening into the nose. Neurogenic inflammation induced by the stimulation of tuft cells at this place resulted in closure of the vomeronasal duct, and this limited entry of potentially hazardous substances to the cavity of the vomeronasal organ (Ogura et al., 2010). In the urinary tract, the ascending of bacteria through the urethra is an important pathway of infection (Wagenlehner et al., 2010, Wagenlehner et al., 2014, Foxman 2014, McLellan et al., 2016). Here, swelling as a result of UTC-induced neurogenic inflammation might delay progress of bacteria into the bladder and deeper into the urinary tract.

After the initial vascular response in neurogenic inflammation, resident immune cells such as mast cells are activated and leukocytes are attracted from the blood stream (Holzer 1998; Steinhoff et al., 2003; Marek-Jozefowicz et al., 2023). This was also the case when neurogenic inflammation was induced by tuft cell stimulation in the mouse nasal cavity also called SCC at this site and trachea (Saunders et al., 2014, Hollenhorst et al., 2022). In the urethra, neither our work nor earlier studies on neurogenic inflammation (Maggi et al., 1987; Pinter et al., 1988; Lundberg et al., 1989; Abelli et al., 1991) have directly examined these immune-related effects, but given the stereotyped nature of this response, they are likely to occur there as well, so that the protective effect of UTC activation may extend beyond the immediate responses occurring during the first minutes.

4.7 Conclusion

The data validate *Chat*-ChR2-EYFP mice, but not *Trpm5*-DREADD mice, as a suitable model for studying UTC function. This model and the use of the bitter tastant denatonium in conjunction with UTC-deficient mice (*Pou2f3*$^{-/-}$) showed that direct

stimulation of UTC leads to the release of neuropeptides (SP) from sensory nerve fibers, most probably through the release of acetylcholine from the activated tuft cells acting on nicotinic receptors on nerve fibers. Thus, UTCs not only trigger long-distance reflexes involving the bladder but also evoke neurogenic inflammation, representing a local defense reaction.

4.8 Limitations of the study

The limitations of the transgenic mouse models used in this study, in particular with regard to the intracellular signaling pathways, have been extensively discussed in the previous chapters and will not be repeated here. Since only the optogenetic model proved to be useful, experiments on intact animals could not be conducted, because LED illumination does not reach the urethral epithelium. Hence, the explanted urethra was chosen for SP release experiments, implying that plasma extravasation, which is dependent on intact circulation, could not be directly measured. Nonetheless, SP release from peptidergic sensory nerve fibers alone is generally accepted as a sufficient indicator of neurogenic inflammation (Holzer 1988) Also, in follow-up experiments of this group in wildtype and *Trmp5*-deficient mice, UTC-induced plasma extravasation in response to intraurethral denatonium was directly shown (Schmidt et al., 2025), further validating the conclusions drawn from the present work. Still, neither this nor previous studies succeeded in identifying a selective chemical activator of naive UTCs, and there is currently no evidence about what the natural physiological stimulus for these cells might be.

Summary

Summary

Brush cells (synonym: tuft cells) are found in the epithelium of the mammalian respiratory, gastrointestinal and urinary tract. They are sensors for hazardous substances, and they release acetylcholine and other mediators (e.g. cysteinyl-leukotrienes and interleukin-25), which activate various cell types including immune cells and nearby sensory nerve fibers. In nose and trachea, these nerve fibers then release the neuropeptide substance P (SP), leading to neurogenic inflammation, a local defense reaction. In the urethra, their stimulation evokes micturition, and previous work of our laboratory using a broadly acting compound also gave first indication of a link of urethral tuft cells (UTC) to neurogenic inflammation. Based on this initial evidence, the present study aims to further investigate their role in inducing neurogenic inflammation by a) establishing a model for the selective activation of brush cells, and b) utilizing a model of brush cell-deficient mice. We used 1) a chemogenetic model, in which brush cells carry a DREADD (designer receptor exclusively activated by designer drugs) 2) an optogenetic approach, using a mouse line (*Chat*-ChR2-EYFP) expressing a fusion protein of the blue light-sensitive ion channel channelrhodopsin-2 (ChR2) and enhanced yellow fluorescent protein (EYFP) expressed under the control of the choline acetyltransferase (*Chat*) promoter, and 3) mice lacking UTC due to genetic deletion of the transcription factor *Pou2f3*. Explanted urethrae from these mouse models were exposed to appropriate stimuli (CNO [clozapine N-oxide] for DREADD, blue LED light for ChR2, denatonium as bitter compound, and capsaicin as UTC-independent activator of nociceptors), and the supernatant was analyzed for content of SP by ELISA. The chemogenetic model proved not to be suitable, since CNO (60 µM) caused SP release also from DREADD control urethrae, likely due to leaky expression of the transgene. In the optogenetic model, UTC-specific expression of the transgene was validated by immunofluorescence with antibodies against the UTC marker DCLK1 (double-cortin like kinase 1) (90% colocalization, 47/52 cells, from 5 animals) and against neuropeptides of sensory nerve fibers (no colocalization). Blue LED light evoked SP release only from urethrae of transgenic but not of control mice. This was fully sensitive to mecamylamine, a general nicotinic acetylcholine receptor inhibitor. The bitter tasting compound denatonium (5 mM) evoked SP release from urethrae of wildtype, but not from urethrae lacking UTC (*Pou2f3*$^{-/-}$), whereas the direct nerve fiber activator capsaicin (1 mM) was equally potent in both strains. The data validate *Chat*-ChR2-EYFP mice, but not *Trpm5*-DREADD mice, as a suitable model for

studying UTC function. This model and the use of the bitter tastant denatonium in conjunction with UTC-deficient mice (*Pou2f3*$^{-/-}$) showed that direct stimulation of UTC leads to the release of neuropeptides (SP) from sensory nerve fibers, most probably through the release of acetylcholine from the activated tuft cells acting on nicotinic receptors on nerve fibers. Thus, UTCs not only trigger long-distance reflexes involving the bladder but also evoke neurogenic inflammation, representing a local defense reaction.

Zusammenfassung

Zusammenfassung

Bürstenzellen kommen im Epithel des respiratorischen, gastrointestinalen und urogenitalen Trakts von Säugetieren vor. Sie fungieren als Sensoren für potenziell schädliche Substanzen und setzen Acetylcholin sowie weitere Mediatoren (z. B. Cysteinyl-Leukotriene und Interleukin-25) frei, welche verschiedene Zelltypen, darunter Immunzellen und benachbarte sensorische Nervenfasern, aktivieren. In Nase und Trachea führen diese Nervenfasern anschließend zur Freisetzung des Neuropeptids Substanz P (SP), was eine neurogene Entzündung als lokale Abwehrreaktion auslöst. In der Urethra bewirkt ihre Stimulation eine Miktion; frühere Arbeiten unserer Arbeitsgruppe unter Verwendung eines breit wirksamen Pharmakons lieferten zudem erste Hinweise auf einen Zusammenhang zwischen urethralen Bürstenzellen (UBC) und neurogener Entzündung.

Aufbauend auf diesen Befunden zielte die vorliegende Studie darauf ab, die Rolle von UBC bei der Entstehung einer neurogenen Entzündung weiter zu untersuchen, indem (a) ein Modell zur selektiven Aktivierung von Bürstenzellen etabliert und (b) Bürstenzell-defiziente Mäuse genutzt wurde. Hierzu wurden eingesetzt: 1) ein chemogenetisches Modell, in dem Bürstenzellen einen DREADD (Designer Receptor Exclusively Activated by Designer Drugs) exprimieren, 2) ein optogenetischer Ansatz unter Verwendung einer Mauslinie (*Chat*-ChR2-EYFP), die ein Fusionsprotein aus dem blaulichtsensitiven Ionenkanal Channelrhodopsin-2 (ChR2) und dem Enhanced Yellow Fluorescent Protein (EYFP) unter der Kontrolle des Cholinacetyltransferase-(*Chat-)*Promotors exprimiert, sowie 3) Mäuse, denen UBC aufgrund der genetischen Deletion des Transkriptionsfaktors Pou2f3 fehlen.

Explantierte Urethren aus diesen Mauslinien wurden geeigneten Stimuli ausgesetzt (CNO [Clozapin-N-Oxid] für DREADD, blaues LED-Licht für ChR2, Denatonium als Bitterstoff und Capsaicin als UTC-unabhängiger Aktivator nozizeptiver Nervenfasern). Anschließend wurde der Überstand mittels ELISA auf seinen Gehalt an SP untersucht. Das chemogenetische Modell erwies sich als ungeeignet, da CNO (60 µM) auch in DREADD-Kontrollurethren eine SP-Freisetzung auslöste, vermutlich aufgrund einer unspezifischen („leaky“) Expression des Transgens. Im optogenetischen Modell wurde die UBC-spezifische Expression des Transgens durch Immunfluoreszenzmarkierungen mit Antikörpern gegen den UBC-Marker DCLK1 (Doublecortin-like Kinase 1) validiert (90 % Kolokalisation, 47/52 Zellen aus 5 Tieren)

sowie mit Antikörpern gegen Neuropeptide sensorischer Nervenfasern, die keine Kolokalisation zeigten. Blaues LED-Licht induzierte eine SP-Freisetzung ausschließlich aus Urethren transgener, nicht jedoch aus Kontrollmäusen. Diese Freisetzung wurde vollständig durch Mecamylamin, einen generellen Inhibitor nikotinischer Acetylcholinrezeptoren, gehemmt. Der Bitterstoff Denatonium (5 mM) induzierte eine SP-Freisetzung aus Urethren von Wildtyp-Mäusen, nicht jedoch aus Urethren von UBC-defizienten Mäusen (*Pou2f3*$^{-/-}$), während der direkte Aktivator sensorischer Nervenfasern Capsaicin (1 mM) in beiden Stämmen gleichermaßen wirksam war.

Die vorliegenden Daten validieren *Chat*-ChR2-EYFP-Mäuse, nicht jedoch *Trpm5*-DREADD-Mäuse, als geeignetes Modell zur Untersuchung der UBC-Funktion. Dieses Modell sowie der Einsatz des Bitterstoffs Denatonium in Kombination mit UBC-defizienten Mäusen (*Pou2f3*$^{-/-}$) zeigen, dass die direkte Stimulation von UBC zur Freisetzung von Neuropeptiden (SP) aus sensorischen Nervenfasern führt, höchstwahrscheinlich vermittelt durch die Freisetzung von Acetylcholin aus aktivierten Bürstenzellen, welches auf nikotinische Rezeptoren der Nervenfasern wirkt. Damit lösen UBC nicht nur Fremdreflexe unter Beteiligung der Harnblase aus, sondern induzieren auch eine neurogene Entzündung als lokale Abwehrreaktion.

References

Abdel Wadood N, Hollenhorst MI, Elhawy MI, Zhao N, Englisch C, Evers SB, Sabachvili M, Maxeiner S, Wyatt A, Herr C, Burkhart AK, Krause E, Yildiz D, Beckmann A, Kusumakshi S, Riethmacher D, Bischoff M, Iden S, Becker SL, Canning BJ, Flockerzi V, Gudermann T, Chubanov V, Bals R, Meier C, Boehm U, Krasteva-Christ G. Tracheal tuft cells release ATP and link innate to adaptive immunity in pneumonia. Nat Commun. 2025 Jan 10;16(1):584. doi: 10.1038/s41467-025-55936-5. PMID: 39794305; PMCID: PMC11724094.

Abelli L, Conte B, Somma V, Parlani M, Geppetti P, Maggi CA. Mechanical irritation induces neurogenic inflammation in the rat urethra. J Urol. 1991 Dec;146(6):1624-6. doi: 10.1016/s0022-5347(17)38200-9. PMID: 1719251.

Adler E, Hoon MA, Mueller KL, Chandrashekar J, Ryba NJ, Zuker CS. A novel family of mammalian taste receptors. Cell. 2000 Mar 17;100(6):693-702. doi: 10.1016/s0092-8674(00)80705-9 . PMID: 10761934 .

Al Lawati H, Blair BM, Larnard J. Urinary Tract Infections: Core Curriculum 2024. Am J Kidney Dis. 2024 Jan;83(1):90-100. doi: 10.1053/j.ajkd.2023.08.009 . Epub 2023 Oct 30. PMID: 37906240 .

Andersson KE. Bladder activation: afferent mechanisms. Urology. 2002 May;59(5 Suppl 1):43-50. doi: 10.1016/s0090-4295(01)01637-5. PMID: 12007522.

Aubron C, Huet O, Ricome S, Borderie D, Pussard E, Leblanc PE, Bouvet O, Vicaut E, Denamur E, Duranteau J. Changes in urine composition after trauma facilitate bacterial growth. BMC Infect Dis. 2012 Nov 29;12:330. doi: 10.1186/1471-2334-12-330. PMID: 23194649; PMCID: PMC3556302.

Bader S, Klein J, Diener M. Choline acetyltransferase and organic cation transporters are responsible for synthesis and propionate-induced release of acetylcholine in colon epithelium. Eur J Pharmacol. 2014 Jun 15;733:23-33. doi: 10.1016/j.ejphar.2014.03.036. Epub 2014 Mar 31. PMID: 24698650.

Bahns E, Ernsberger U, Jänig W, Nelke A. Functional characteristics of lumbar visceral afferent fibres from the urinary bladder and the urethra in the cat. Pflugers Arch. 1986 Nov;407(5):510-8. doi: 10.1007/BF00657509. PMID: 3786110.

Bankova LG, Dwyer DF, Yoshimoto E, Ualiyeva S, McGinty JW, Raff H, von Moltke J, Kanaoka Y, Frank Austen K, Barrett NA. The cysteinyl leukotriene 3 receptor regulates expansion of IL-25-producing airway brush cells leading to type 2 inflammation. Sci Immunol. 2018 Oct 5;3(28):eaat9453. doi: 10.1126/sciimmunol.aat9453. PMID: 30291131; PMCID: PMC6599626.

Bejanin S, Cervini R, Mallet J, Berrard S. A unique gene organization for two cholinergic markers, choline acetyltransferase and a putative vesicular transporter of acetylcholine. J Biol Chem. 1994 Sep 2;269(35):21944-7. PMID: 8071313.

Bellier JP, Kimura H. Acetylcholine synthesis by choline acetyltransferase of a peripheral type as demonstrated in adult rat dorsal root ganglion. J Neurochem. 2007 Jun;101(6):1607-18. doi: 10.1111/j.1471-4159.2007.04458.x. PMID: 17542812.

References

Bellier JP, Kimura H. Peripheral type of choline acetyltransferase: biological and evolutionary implications for novel mechanisms in cholinergic system. J Chem Neuroanat. 2011 Dec;42(4):225-35. doi: 10.1016/j.jchemneu.2011.02.005. Epub 2011 Mar 5. PMID: 21382474.

Billipp TE, Fung C, Webeck LM, Sargent DB, Gologorsky MB, Chen Z, McDaniel MM, Kasal DN, McGinty JW, Barrow KA, Rich LM, Barilli A, Sabat M, Debley JS, Wu C, Myers R, Howitt MR, von Moltke J. Tuft cell-derived acetylcholine promotes epithelial chloride secretion and intestinal helminth clearance. Immunity. 2024 Jun 11;57(6):1243-1259.e8. doi: 10.1016/j.immuni.2024.03.023. Epub 2024 May 13. PMID: 38744291; PMCID: PMC11168877.

Boyden ES, Zhang F, Bamberg E, Nagel G, Deisseroth K. Millisecond-timescale, genetically targeted optical control of neural activity. Nat Neurosci. 2005 Sep;8(9):1263-8. doi: 10.1038/nn1525. Epub 2005 Aug 14. PMID: 16116447.

Bradley W, Griffin D, Teague C, Timm G. Sensory innervation of the mammalian urethra. Invest Urol. 1973 Jan;10(4):287-9. PMID: 4683378.

Brain SD. Sensory neuropeptides: their role in inflammation and wound healing. Immunopharmacology. 1997 Oct;37(2-3):133-52. doi: 10.1016/s0162-3109(97)00055-6. PMID: 9403332.

Briand L, Salles C. (2016). Taste perception and integration. In Flavor: From Food to Behaviors, Wellbeing and Health, (S. 101–119). Cambridge, UK: Woodhead Publishing.

Briand, Loïc; Salles, Christian (2016): Taste perception and integration. In : Flavor: Elsevier, pp. 101–119.

Brokaw JJ, White GW. Calcitonin gene-related peptide potentiates substance P-induced plasma extravasation in the rat trachea. Lung. 1992;170(2):85-93. doi: 10.1007/BF00175980. PMID: 1380110.

Brown PD, Foxman B. Pathogenesis of Urinary Tract Infection: the Role of Sexual Behavior and Sexual Transmission. Curr Infect Dis Rep. 2000 Dec;2(6):513-517. doi: 10.1007/s11908-000-0054-4. PMID: 11095901.

Brown TC, Bond CE, Hoover DB. Variable expression of GFP in different populations of peripheral cholinergic neurons of ChAT^{BAC}-eGFP transgenic mice. Auton Neurosci. 2018 Mar;210:44-54. doi: 10.1016/j.autneu.2017.12.005. Epub 2017 Dec 20. PMID: 29288022; PMCID: PMC5878110.

Bruce N. 1910. Über die Beziehung der sensiblen Nervenendigungen zum Entzündungsvorgang. Archiv für experimentelle Pathologie und Pharmakologie, (63):424–433.

Bruce N. 1913. Vasodilator Axon-reflexes. Quarterly journal of experimental physiology, (6):339–354.

Burnstock G. P2X receptors in sensory neurones. Br J Anaesth. 2000 Apr;84(4):476-88. doi: 10.1093/oxfordjournals.bja.a013473. PMID: 10823099.

Caceres AI, Brackmann M, Elia MD, Bessac BF, del Camino D, D'Amours M, Witek JS, Fanger CM, Chong JA, Hayward NJ, Homer RJ, Cohn L, Huang X, Moran MM, Jordt SE. A sensory neuronal ion channel essential for airway inflammation and hyperreactivity in asthma. Proc Natl Acad Sci U S A. 2009 Jun 2;106(22):9099-104. doi: 10.1073/pnas.0900591106. Epub 2009 May 19. PMID: 19458046; PMCID: PMC2684498.

References

Caterina MJ, Schumacher MA, Tominaga M, Rosen TA, Levine JD, Julius D. The capsaicin receptor: a heat-activated ion channel in the pain pathway. Nature. 1997 Oct 23;389(6653):816-24. doi: 10.1038/39807. PMID: 9349813.

Chandrashekar J, Mueller KL, Hoon MA, Adler E, Feng L, Guo W, Zuker CS, Ryba NJ. T2Rs function as bitter taste receptors. Cell. 2000 Mar 17;100(6):703-11. doi: 10.1016/s0092-8674(00)80706-0. PMID: 10761935.

Chu DQ, Choy M, Foster P, Cao T, Brain SD. A comparative study of the ability of calcitonin gene-related peptide and adrenomedullin(13 - 52) to modulate microvascular but not thermal hyperalgesia responses. Br J Pharmacol. 2000 Aug;130(7):1589-96. doi: 10.1038/sj.bjp.0703502. PMID: 10928962; PMCID: PMC1572244.

Coli A, Gao S, Kaestner L. Sodium-Selective Channelrhodopsins. Cells. 2024 Nov 8;13(22):1852. doi: 10.3390/cells13221852. PMID: 39594600; PMCID: PMC11592924.

Cyphert JM, Kovarova M, Allen IC, Hartney JM, Murphy DL, Wess J, Koller BH. Cooperation between mast cells and neurons is essential for antigen-mediated bronchoconstriction. J Immunol. 2009 Jun 15;182(12):7430-9. doi: 10.4049/jimmunol.0900039. PMID: 19494266; PMCID: PMC3901060.

Dai L. Non-neuronal acetylcholine as a spatiotemporal autacoid in the immune and circulatory systems. Int Immunopharmacol. 2025 Nov 14;165:115414. doi: 10.1016/j.intimp.2025.115414. Epub 2025 Aug 28. PMID: 40882547.

Dale HH. On some physiological actions of ergot. J Physiol. 1906 May 31;34(3):163-206. doi: 10.1113/jphysiol.1906.sp001148. PMID: 16992821; PMCID: PMC1465771.

Damak S, Rong M, Yasumatsu K, Kokrashvili Z, Pérez CA, Shigemura N, Yoshida R, Mosinger B Jr, Glendinning JI, Ninomiya Y, Margolskee RF. Trpm5 null mice respond to bitter, sweet, and umami compounds. Chem Senses. 2006 Mar;31(3):253-64. doi: 10.1093/chemse/bjj027. Epub 2006 Jan 25. PMID: 16436689.

de Groat WC, Griffiths D, Yoshimura N. Neural control of the lower urinary tract. Compr Physiol. 2015 Jan;5(1):327-96. doi: 10.1002/cphy.c130056. PMID: 25589273; PMCID: PMC4480926.

Deckmann K, Filipski K, Krasteva-Christ G, Fronius M, Althaus M, Rafiq A, Papadakis T, Renno L, Jurastow I, Wessels L, Wolff M, Schütz B, Weihe E, Chubanov V, Gudermann T, Klein J, Bschleipfer T, Kummer W. Bitter triggers acetylcholine release from polymodal urethral chemosensory cells and bladder reflexes. Proc Natl Acad Sci U S A. 2014 Jun 3;111(22):8287-92. doi: 10.1073/pnas.1402436111. Epub 2014 May 19. PMID: 24843119; PMCID: PMC4050540.

Deckmann K, Krasteva-Christ G, Rafiq A, Herden C, Wichmann J, Knauf S, Nassenstein C, Grevelding CG, Dorresteijn A, Chubanov V, Gudermann T, Bschleipfer T, Kummer W. Cholinergic urethral brush cells are widespread throughout placental mammals. Int Immunopharmacol. 2015 Nov;29(1):51-6. doi: 10.1016/j.intimp.2015.05.038. Epub 2015 Jun 1. PMID: 26044348.

Deckmann K, Rafiq A, Erdmann C, Illig C, Durschnabel M, Wess J, Weidner W, Bschleipfer T, Kummer W. Muscarinic receptors 2 and 5 regulate bitter response of urethral brush cells via negative feedback. FASEB J. 2018 Jun;32(6):2903-2910. doi: 10.1096/fj.201700582R. Epub 2018 Jan 17. PMID: 29401598; PMCID: PMC6137718.

Devor M, Papir-Kricheli D, Nachmias E, Rosenthal F, Gilon C, Chorev M, Selinger Z. Substance P-induced cutaneous plasma extravasation in rats is mediated by NK-1 tachykinin receptors. Neurosci Lett. 1989 Aug 28;103(2):203-8. doi: 10.1016/0304-3940(89)90576-4. PMID: 2475833.

References

Ding W, Stohl LL, Wagner JA, Granstein RD. Calcitonin gene-related peptide biases Langerhans cells toward Th2-type immunity. J Immunol. 2008 Nov 1;181(9):6020-6. doi: 10.4049/jimmunol.181.9.6020. PMID: 18941191; PMCID: PMC2679684.

Drurey C, Lindholm HT, Coakley G, Poveda MC, Löser S, Doolan R, Gerbe F, Jay P, Harris N, Oudhoff MJ, Maizels RM. Intestinal epithelial tuft cell induction is negated by a murine helminth and its secreted products. J Exp Med. 2022 Jan 3;219(1):e20211140. doi: 10.1084/jem.20211140. Epub 2021 Nov 15. PMID: 34779829; PMCID: PMC8597987.

Dubin AE, Patapoutian A. Nociceptors: the sensors of the pain pathway. J Clin Invest. 2010 Nov;120(11):3760-72. doi: 10.1172/JCI42843. Epub 2010 Nov 1. PMID: 21041958; PMCID: PMC2964977.

Erickson JD, Varoqui H, Schäfer MK, Modi W, Diebler MF, Weihe E, Rand J, Eiden LE, Bonner TI, Usdin TB. Functional identification of a vesicular acetylcholine transporter and its expression from a "cholinergic" gene locus. J Biol Chem. 1994 Sep 2;269(35):21929-32. PMID: 8071310.

Everaerts W, Gees M, Alpizar YA, Farre R, Leten C, Apetrei A, Dewachter I, van Leuven F, Vennekens R, De Ridder D, Nilius B, Voets T, Talavera K. The capsaicin receptor TRPV1 is a crucial mediator of the noxious effects of mustard oil. Curr Biol. 2011 Feb 22;21(4):316-21. doi: 10.1016/j.cub.2011.01.031 . PMID: 21315593 .

Feber JL, van Asselt E, van Mastrigt R. Neurophysiological modeling of voiding in rats: urethral nerve response to urethral pressure and flow. Am J Physiol. 1998 May;274(5):R1473-81. doi: 10.1152/ajpregu.1998.274.5.R1473. PMID: 9612416.

Ferreira A, Duarte Cruz C. The urethra in continence and sensation: Neural aspects of urethral function. Neurourol Urodyn. 2021 Mar;40(3):744-752. doi: 10.1002/nau.24632. Epub 2021 Feb 19. PMID: 33604909.

Finger TE, Böttger B, Hansen A, Anderson KT, Alimohammadi H, Silver WL. Solitary chemoreceptor cells in the nasal cavity serve as sentinels of respiration. Proc Natl Acad Sci U S A. 2003 Jul 22;100(15):8981-6. doi: 10.1073/pnas.1531172100. Epub 2003 Jul 11. PMID: 12857948; PMCID: PMC166424.

Flores-Mireles AL, Walker JN, Caparon M, Hultgren SJ. Urinary tract infections: epidemiology, mechanisms of infection and treatment options. Nat Rev Microbiol. 2015 May;13(5):269-84. doi: 10.1038/nrmicro3432. Epub 2015 Apr 8. PMID: 25853778; PMCID: PMC4457377.

Floyd K, Hick VE, Morrison JF. Mechanosensitive afferent units in the hypogastric nerve of the cat. J Physiol. 1976 Jul;259(2):457-71. doi: 10.1113/jphysiol.1976.sp011476. PMID: 986462; PMCID: PMC1309039.

Foxman B, Brown P. Epidemiology of urinary tract infections: transmission and risk factors, incidence, and costs. Infect Dis Clin North Am. 2003 Jun;17(2):227-41. doi: 10.1016/s0891-5520(03)00005-9. PMID: 12848468.

Foxman B. Epidemiology of urinary tract infections: incidence, morbidity, and economic costs. Am J Med. 2002 Jul 8;113 Suppl 1A:5S-13S. doi: 10.1016/s0002-9343(02)01054-9. PMID: 12113866.

Foxman B. Urinary tract infection syndromes: occurrence, recurrence, bacteriology, risk factors, and disease burden. Infect Dis Clin North Am. 2014 Mar;28(1):1-13. doi: 10.1016/j.idc.2013.09.003. Epub 2013 Dec 8. PMID: 24484571.

References

Fujii T, Takada-Takatori Y, Horiguchi K, Kawashima K. Mediatophore regulates acetylcholine release from T cells. J Neuroimmunol. 2012 Mar;244(1-2):16-22. doi: 10.1016/j.jneuroim.2011.12.022. Epub 2012 Jan 14. PMID: 22245286.

Gamage R, Zaborszky L, Münch G, Gyengesi E. Evaluation of eGFP expression in the ChAT-eGFP transgenic mouse brain. BMC Neurosci. 2023 Jan 17;24(1):4. doi: 10.1186/s12868-023-00773-9. PMID: 36650430; PMCID: PMC9847127.

Gerbe F, Legraverend C, Jay P. The intestinal epithelium tuft cells: specification and function. Cell Mol Life Sci. 2012 Sep;69(17):2907-17. doi: 10.1007/s00018-012-0984-7. Epub 2012 Apr 19. PMID: 22527717; PMCID: PMC3417095.

Gerbe F, Sidot E, Smyth DJ, Ohmoto M, Matsumoto I, Dardalhon V, Cesses P, Garnier L, Pouzolles M, Brulin B, Bruschi M, Harcus Y, Zimmermann VS, Taylor N, Maizels RM, Jay P. Intestinal epithelial tuft cells initiate type 2 mucosal immunity to helminth parasites. Nature. 2016 Jan 14;529(7585):226-30. doi: 10.1038/nature16527. PMID: 26762460; PMCID: PMC7614903.

Gläske G, Schicktanz C. 2016. BARMER GEK Arzneimittelreport 2014. Berlin, Deutschland: Barmer GEK.

Gomez-Sanchez JA, Pilch KS, van der Lans M, Fazal SV, Benito C, Wagstaff LJ, Mirsky R, Jessen KR. After Nerve Injury, Lineage Tracing Shows That Myelin and Remak Schwann Cells Elongate Extensively and Branch to Form Repair Schwann Cells, Which Shorten Radically on Remyelination. J Neurosci. 2017 Sep 13;37(37):9086-9099. doi: 10.1523/JNEUROSCI.1453-17.2017. Epub 2017 Aug 3. PMID: 28904214; PMCID: PMC5597985.

Gulbransen B, Silver W, Finger TE. Solitary chemoreceptor cell survival is independent of intact trigeminal innervation. J Comp Neurol. 2008 May 1;508(1):62-71. doi: 10.1002/cne.21657. PMID: 18300260; PMCID: PMC2586644.

Gulbransen BD, Clapp TR, Finger TE, Kinnamon SC. Nasal solitary chemoreceptor cell responses to bitter and trigeminal stimulants in vitro. J Neurophysiol. 2008 Jun;99(6):2929-37. doi: 10.1152/jn.00066.2008. Epub 2008 Apr 16. PMID: 18417634; PMCID: PMC2765583.

Höfer D, Drenckhahn D. Identification of brush cells in the alimentary and respiratory system by antibodies to villin and fimbrin. Histochemistry. 1992 Nov;98(4):237-42. doi: 10.1007/BF00271037. PMID: 1459863.

Höfer D, Drenckhahn D. Identification of the taste cell G-protein, alpha-gustducin, in brush cells of the rat pancreatic duct system. Histochem Cell Biol. 1998 Sep;110(3):303-9. doi: 10.1007/s004180050292. PMID: 9749964.

Höfer D, Püschel B, Drenckhahn D. Taste receptor-like cells in the rat gut identified by expression of alpha-gustducin. Proc Natl Acad Sci U S A. 1996 Jun 25;93(13):6631-4. doi: 10.1073/pnas.93.13.6631. PMID: 8692869; PMCID: PMC39077.

Höfer, D.; Drenckhahn, D. (1992): Identification of brush cells in the alimentary and respiratory system by antibodies to villin and fimbrin. In *Histochemistry* 98 (4), pp. 237–242. DOI: 10.1007/BF00271037.

Hollenhorst MI, Krasteva-Christ G. Chemosensory cells in the respiratory tract as crucial regulators of innate immune responses. J Physiol. 2023 May;601(9):1555-1572. doi: 10.1113/JP282307. Epub 2023 Apr 9. PMID: 37009787.

References

Hollenhorst MI, Nandigama R, Evers SB, Gamayun I, Abdel Wadood N, Salah A, Pieper M, Wyatt A, Stukalov A, Gebhardt A, Nadolni W, Burow W, Herr C, Beisswenger C, Kusumakshi S, Ectors F, Kichko TI, Hübner L, Reeh P, Munder A, Wienhold SM, Witzenrath M, Bals R, Flockerzi V, Gudermann T, Bischoff M, Lipp P, Zierler S, Chubanov V, Pichlmair A, König P, Boehm U, Krasteva-Christ G. Bitter taste signaling in tracheal epithelial brush cells elicits innate immune responses to bacterial infection. J Clin Invest. 2022 Jul 1;132(13):e150951. doi: 10.1172/JCI150951. PMID: 35503420; PMCID: PMC9246383.

Holzer P. Local effector functions of capsaicin-sensitive sensory nerve endings: involvement of tachykinins, calcitonin gene-related peptide and other neuropeptides. Neuroscience. 1988 Mar;24(3):739-68. doi: 10.1016/0306-4522(88)90064-4. PMID: 3288903.

Holzer P. Neurogenic vasodilatation and plasma leakage in the skin. Gen Pharmacol. 1998 Jan;30(1):5-11. doi: 10.1016/s0306-3623(97)00078-5. PMID: 9457475.

Holzer P. Peptidergic sensory neurons in the control of vascular functions: mechanisms and significance in the cutaneous and splanchnic vascular beds. Rev Physiol Biochem Pharmacol. 1992;121:49-146. doi: 10.1007/BFb0033194. PMID: 1485073.

Holzer, P. (1994). *Local Effector Functions of Primary Afferent Nerve Fibres.* In: L. Urban (Ed.) *Cellular Mechanisms of Sensory Processing. The Somatosensory System*. NATO ASI Subseries H: Vol. 79, pp. 133-147.

Hosoi J, Murphy GF, Egan CL, Lerner EA, Grabbe S, Asahina A, Granstein RD. Regulation of Langerhans cell function by nerves containing calcitonin gene-related peptide. Nature. 1993 May 13;363(6425):159-63. doi: 10.1038/363159a0. PMID: 8483499.

Howitt MR, Lavoie S, Michaud M, Blum AM, Tran SV, Weinstock JV, Gallini CA, Redding K, Margolskee RF, Osborne LC, Artis D, Garrett WS. Tuft cells, taste-chemosensory cells, orchestrate parasite type 2 immunity in the gut. Science. 2016 Mar 18;351(6279):1329-33. doi: 10.1126/science.aaf1648. Epub 2016 Feb 4. PMID: 26847546; PMCID: PMC5528851.

Israël M, Lesbats B, Morel N, Manaranche R, Birman S. The lipid requirements of mediatophore for acetylcholine release activity. Large-scale purification of this protein in a reactive form. Neurochem Int. 1988;13(2):199-205. doi: 10.1016/0197-0186(88)90055-1. PMID: 20501288.

Jung SY, Fraser MO, Ozawa H, Yokoyama O, Yoshiyama M, De Groat WC, Chancellor MB. Urethral afferent nerve activity affects the micturition reflex; implication for the relationship between stress incontinence and detrusor instability. J Urol. 1999 Jul;162(1):204-12. doi: 10.1097/00005392-199907000-00069. PMID: 10379788.

Kandel C, Schmidt P, Perniss A, Keshavarz M, Scholz P, Osterloh S, Althaus M, Kummer W, Deckmann K. ENaC in Cholinergic Brush Cells. Front Cell Dev Biol. 2018 Aug 15;6:89. doi: 10.3389/fcell.2018.00089. PMID: 30159312; PMCID: PMC6103785.

Kaske S, Krasteva G, König P, Kummer W, Hofmann T, Gudermann T, Chubanov V. TRPM5, a taste-signaling transient receptor potential ion-channel, is a ubiquitous signaling component in chemosensory cells. BMC Neurosci. 2007 Jul 4;8:49. doi: 10.1186/1471-2202-8-49. PMID: 17610722; PMCID: PMC1931605.

Kennelly MJ, Arena KC, Shaffer N, Bennett ME, Grill WM, Grill JH, Boggs JW. Electrical stimulation of the urethra evokes bladder contractions in a woman with spinal cord injury. J Spinal Cord Med. 2010;33(3):261-5. doi: 10.1080/10790268.2010.11689704. PMID: 20737800; PMCID: PMC2920120.

References

Kennelly MJ, Bennett ME, Grill WM, Grill JH, Boggs JW. Electrical stimulation of the urethra evokes bladder contractions and emptying in spinal cord injury men: case studies. J Spinal Cord Med. 2011;34(3):315-21. doi: 10.1179/2045772311Y.0000000012. PMID: 21756572; PMCID: PMC3127369.

Keshavarz M, Faraj Tabrizi S, Ruppert AL, Pfeil U, Schreiber Y, Klein J, Brandenburger I, Lochnit G, Bhushan S, Perniss A, Deckmann K, Hartmann P, Meiners M, Mermer P, Rafiq A, Winterberg S, Papadakis T, Thomas D, Angioni C, Oberwinkler J, Chubanov V, Gudermann T, Gärtner U, Offermanns S, Schütz B, Kummer W. Cysteinyl leukotrienes and acetylcholine are biliary tuft cell cotransmitters. Sci Immunol. 2022 Mar 4;7(69):eabf6734. doi: 10.1126/sciimmunol.abf6734. Epub 2022 Mar 4. PMID: 35245090.

Kinnamon S, Finger T. The Role of ATP and Purinergic Receptors in Taste Signaling. Handb Exp Pharmacol. 2022;275:91-107. doi: 10.1007/164_2021_518. PMID: 34435233; PMCID: PMC10078839.

Kirjavainen PV, Pautler S, Baroja ML, Anukam K, Crowley K, Carter K, Reid G. Abnormal immunological profile and vaginal microbiota in women prone to urinary tract infections. Clin Vaccine Immunol. 2009 Jan;16(1):29-36. doi: 10.1128/CVI.00323-08 . Epub 2008 Nov 19. PMID: 19020112 ; PMCID: PMC2620669.

Kohler TS, Yadven M, Manvar A, Liu N, Monga M. The length of the male urethra. Int Braz J Urol. 2008 Jul-Aug;34(4):451-4; discussion 455-6. doi: 10.1590/s1677-55382008000400007. PMID: 18778496.

Kolisnyk B, Guzman MS, Raulic S, Fan J, Magalhães AC, Feng G, Gros R, Prado VF, Prado MA. ChAT-ChR2-EYFP mice have enhanced motor endurance but show deficits in attention and several additional cognitive domains. J Neurosci. 2013 Jun 19;33(25):10427-38. doi: 10.1523/JNEUROSCI.0395-13.2013. PMID: 23785154; PMCID: PMC6618591.

Kranz J, Schmidt S, Naber K. 2017. S3-Leitlinie: Unkomplizierte Harnwegsinfektionen. Bayerisches Ärzteblatt, (11):1–8.

Krasteva G, Canning BJ, Hartmann P, Veres TZ, Papadakis T, Mühlfeld C, Schliecker K, Tallini YN, Braun A, Hackstein H, Baal N, Weihe E, Schütz B, Kotlikoff M, Ibanez-Tallon I, Kummer W. Cholinergic chemosensory cells in the trachea regulate breathing. Proc Natl Acad Sci U S A. 2011 Jun 7;108(23):9478-83. doi: 10.1073/pnas.1019418108. Epub 2011 May 23. PMID: 21606356; PMCID: PMC3111311.

Krasteva G, Hartmann P, Papadakis T, Bodenbenner M, Wessels L, Weihe E, Schütz B, Langheinrich AC, Chubanov V, Gudermann T, Ibanez-Tallon I, Kummer W. Cholinergic chemosensory cells in the auditory tube. Histochem Cell Biol. 2012 Apr;137(4):483-97. doi: 10.1007/s00418-012-0911-x. Epub 2012 Jan 20. PMID: 22261922.

Kummer W, Krasteva-Christ G. Non-neuronal cholinergic airway epithelium biology. Curr Opin Pharmacol. 2014 Jun;16:43-9. doi: 10.1016/j.coph.2014.03.001. Epub 2014 Mar 27. PMID: 24681350.

Kummer W, Lips KS, Pfeil U. The epithelial cholinergic system of the airways. Histochem Cell Biol. 2008 Aug;130(2):219-34. doi: 10.1007/s00418-008-0455-2. Epub 2008 Jun 20. PMID: 18566825; PMCID: PMC2491704.

References

Lasconi C, Pifferi S, Hernandez-Clavijo A, Merigo F, Cecchini MP, Gonzalez-Velandia KY, Agostinelli E, Sbarbati A, Menini A. Bitter tastants and artificial sweeteners activate a subset of epithelial cells in acute tissue slices of the rat trachea. Sci Rep. 2019 Jun 20;9(1):8834. doi: 10.1038/s41598-019-45456-w . PMID: 31222082 ; PMCID: PMC6586933.

Le Grevès P, Nyberg F, Hökfelt T, Terenius L. Calcitonin gene-related peptide is metabolized by an endopeptidase hydrolyzing substance P. Regul Pept. 1989 Jun-Jul;25(3):277-86. doi: 10.1016/0167-0115(89)90176-6. PMID: 2475892.

Lee RJ, Kofonow JM, Rosen PL, Siebert AP, Chen B, Doghramji L, Xiong G, Adappa ND, Palmer JN, Kennedy DW, Kreindler JL, Margolskee RF, Cohen NA. Bitter and sweet taste receptors regulate human upper respiratory innate immunity. J Clin Invest. 2014 Mar;124(3):1393-405. doi: 10.1172/JCI72094. Epub 2014 Feb 17. PMID: 24531552; PMCID: PMC3934184.

Lembeck F. 1953. Zur Frage der zentralen Übertragung afferenter Impulse - III. Mitteilung. Das Vorkommen und die Bedeutung der Substanz P in den dorsalen Wurzeln des Rückenmarks. Archiv für Experimentelle Pathologie und Pharmakologie, 219(1–2):197–213.

Levine JD, Clark R, Devor M, Helms C, Moskowitz MA, Basbaum AI. Intraneuronal substance P contributes to the severity of experimental arthritis. Science. 1984 Nov 2;226(4674):547-9. doi: 10.1126/science.6208609. PMID: 6208609.

Levy MM, Artigas A, Phillips GS, Rhodes A, Beale R, Osborn T, Vincent JL, Townsend S, Lemeshow S, Dellinger RP. Outcomes of the Surviving Sepsis Campaign in intensive care units in the USA and Europe: a prospective cohort study. Lancet Infect Dis. 2012 Dec;12(12):919-24. doi: 10.1016/S1473-3099(12)70239-6. Epub 2012 Oct 26. PMID: 23103175.

Lewis T. The Blood Vessels of the Human Skin. Br Med J. 1927 Jul 10;2(3418):61-2. doi: 10.1136/bmj.2.3418.61. PMID: 20772665; PMCID: PMC2522949.

Lin JY. A user's guide to channelrhodopsin variants: features, limitations and future developments. Exp Physiol. 2011 Jan;96(1):19-25. doi: 10.1113/expphysiol.2009.051961. Epub 2010 Jul 9. PMID: 20621963; PMCID: PMC2995811.

Lips KS, Volk C, Schmitt BM, Pfeil U, Arndt P, Miska D, Ermert L, Kummer W, Koepsell H. Polyspecific cation transporters mediate luminal release of acetylcholine from bronchial epithelium. Am J Respir Cell Mol Biol. 2005 Jul;33(1):79-88. doi: 10.1165/rcmb.2004-0363OC. Epub 2005 Apr 7. PMID: 15817714.

Loewi, O. Über humorale übertragbarkeit der Herznervenwirkung. *Pflügers Arch*. **189**, 239–242 (1921). https://doi.org/10.1007/BF01738910

Lossow K, Hübner S, Roudnitzky N, Slack JP, Pollastro F, Behrens M, Meyerhof W. Comprehensive Analysis of Mouse Bitter Taste Receptors Reveals Different Molecular Receptive Ranges for Orthologous Receptors in Mice and Humans. J Biol Chem. 2016 Jul 15;291(29):15358-77. doi: 10.1074/jbc.M116.718544. Epub 2016 May 20. PMID: 27226572; PMCID: PMC4946946.

Luciano L, Reale E. Presence of brush cells in the mouse gallbladder. Microsc Res Tech. 1997 Sep 15;38(6):598-608. doi: 10.1002/(SICI)1097-0029(19970915)38:6<598::AID-JEMT4>3.0.CO;2-B. PMID: 9330348.

Lundberg JM, Hökfelt T, Martling CR, Saria A, Cuello C. Substance P-immunoreactive sensory nerves in the lower respiratory tract of various mammals including man. Cell Tissue Res. 1984;235(2):251-61. doi: 10.1007/BF00217848. PMID: 6200231.

References

Maggi CA, Santicioli P, Abelli L, Parlani M, Capasso M, Conte B, Giuliani S, Meli A. Regional differences in the effects of capsaicin and tachykinins on motor activity and vascular permeability of the rat lower urinary tract. Naunyn Schmiedebergs Arch Pharmacol. 1987 Jun;335(6):636-45. doi: 10.1007/BF00166980. PMID: 2442629.

Mahmoud W, Perniss A, Poharkar K, Keshavarz M, Gärtner U, Oberwinkler J, Schütz B, Worzfeld T, Offermanns S, Kummer W. Differential expression of villin and advillin by neuroendocrine and tuft cells in the murine lower airways. Cell Tissue Res. 2025 Oct;402(1):1-20. doi: 10.1007/s00441-025-04003-y. Epub 2025 Sep 1. PMID: 40888895; PMCID: PMC12484096.

Mancuso G, Midiri A, Gerace E, Marra M, Zummo S, Biondo C. Urinary Tract Infections: The Current Scenario and Future Prospects. Pathogens. 2023 Apr 20;12(4):623. doi: 10.3390/pathogens12040623. PMID: 37111509; PMCID: PMC10145414.

Mantyh PW. Neurobiology of substance P and the NK1 receptor. J Clin Psychiatry. 2002;63 Suppl 11:6-10. PMID: 12562137.

Marek-Jozefowicz L, Nedoszytko B, Grochocka M, Żmijewski MA, Czajkowski R, Cubała WJ, Slominski AT. Molecular Mechanisms of Neurogenic Inflammation of the Skin. Int J Mol Sci. 2023 Mar 5;24(5):5001. doi: 10.3390/ijms24055001. PMID: 36902434; PMCID: PMC10003326.

Maurer B, Graf N, Michel BA, Müller-Ladner U, Czirják L, Denton CP, Tyndall A, Metzig C, Lanius V, Khanna D, Distler O; EUSTAR co-authors. Prediction of worsening of skin fibrosis in patients with diffuse cutaneous systemic sclerosis using the EUSTAR database. Ann Rheum Dis. 2015 Jun;74(6):1124-31. doi: 10.1136/annrheumdis-2014-205226. Epub 2014 Jun 30. PMID: 24981642.

McGee MJ, Grill WM. Selective co-stimulation of pudendal afferents enhances bladder activation and improves voiding efficiency. Neurourol Urodyn. 2014 Nov;33(8):1272-8. doi: 10.1002/nau.22474. Epub 2013 Aug 9. PMID: 23934615; PMCID: PMC4282936.

McGinty JW, Ting HA, Billipp TE, Nadjsombati MS, Khan DM, Barrett NA, Liang HE, Matsumoto I, von Moltke J. Tuft-Cell-Derived Leukotrienes Drive Rapid Anti-helminth Immunity in the Small Intestine but Are Dispensable for Anti-protist Immunity. Immunity. 2020 Mar 17;52(3):528-541.e7. doi: 10.1016/j.immuni.2020.02.005. Epub 2020 Mar 10. PMID: 32160525; PMCID: PMC7469474.

McLatchie LM, Fraser NJ, Main MJ, Wise A, Brown J, Thompson N, Solari R, Lee MG, Foord SM. RAMPs regulate the transport and ligand specificity of the calcitonin-receptor-like receptor. Nature. 1998 May 28;393(6683):333-9. doi: 10.1038/30666. PMID: 9620797.

McLaughlin SK, McKinnon PJ, Margolskee RF. Gustducin is a taste-cell-specific G protein closely related to the transducins. Nature. 1992 Jun 18;357(6379):563-9. doi: 10.1038/357563a0. PMID: 1608467.

Measley RE Jr, Levison ME. Host defense mechanisms in the pathogenesis of urinary tract infection. Med Clin North Am. 1991 Mar;75(2):275-86. doi: 10.1016/s0025-7125(16)30453-9. PMID: 1996033.

Meyerhof W, Batram C, Kuhn C, Brockhoff A, Chudoba E, Bufe B, Appendino G, Behrens M. The molecular receptive ranges of human TAS2R bitter taste receptors. Chem Senses. 2010 Feb;35(2):157-70. doi: 10.1093/chemse/bjp092. Epub 2009 Dec 18. PMID: 20022913.

Middelhoff M, Westphalen CB, Hayakawa Y, Yan KS, Gershon MD, Wang TC, Quante M. Dclk1-expressing tuft cells: critical modulators of the intestinal niche? Am J Physiol Gastrointest Liver

References

Physiol. 2017 Oct 1;313(4):G285-G299. doi: 10.1152/ajpgi.00073.2017. Epub 2017 Jul 6. PMID: 28684459; PMCID: PMC5668570.

Mikami N, Matsushita H, Kato T, Kawasaki R, Sawazaki T, Kishimoto T, Ogitani Y, Watanabe K, Miyagi Y, Sueda K, Fukada S, Yamamoto H, Tsujikawa K. Calcitonin gene-related peptide is an important regulator of cutaneous immunity: effect on dendritic cell and T cell functions. J Immunol. 2011 Jun 15;186(12):6886-93. doi: 10.4049/jimmunol.1100028. Epub 2011 May 6. PMID: 21551361.

Nadjsombati MS, McGinty JW, Lyons-Cohen MR, Jaffe JB, DiPeso L, Schneider C, Miller CN, Pollack JL, Nagana Gowda GA, Fontana MF, Erle DJ, Anderson MS, Locksley RM, Raftery D, von Moltke J. Detection of Succinate by Intestinal Tuft Cells Triggers a Type 2 Innate Immune Circuit. Immunity. 2018 Jul 17;49(1):33-41.e7. doi: 10.1016/j.immuni.2018.06.016. PMID: 30021144; PMCID: PMC6084797.

Nagel G, Szellas T, Huhn W, Kateriya S, Adeishvili N, Berthold P, Ollig D, Hegemann P, Bamberg E. Channelrhodopsin-2, a directly light-gated cation-selective membrane channel. Proc Natl Acad Sci U S A. 2003 Nov 25;100(24):13940-5. doi: 10.1073/pnas.1936192100. Epub 2003 Nov 13. PMID: 14615590; PMCID: PMC283525.

Nandigama R, Ibañez-Tallon I, Lips KS, Schwantes U, Kummer W, Bschleipfer T. Expression of nicotinic acetylcholine receptor subunit mRNA in mouse bladder afferent neurons. Neuroscience. 2013 Jan 15;229:27-35. doi: 10.1016/j.neuroscience.2012.10.059. Epub 2012 Nov 3. PMID: 23131712.

Ndjim M, Gasmi I, Herbert F, Joséphine C, Bas J, Lamrani A, Coutry N, Henry S, Zimmermann VS, Dardalhon V, Campillo Poveda M, Turtoi E, Thirard S, Forichon L, Giordano A, Ciancia C, Homayed Z, Pannequin J, Britton C, Devaney E, McNeilly TN, Berrard S, Turtoi A, Maizels RM, Gerbe F, Jay P. Tuft cell acetylcholine is released into the gut lumen to promote anti-helminth immunity. Immunity. 2024 Jun 11;57(6):1260-1273.e7. doi: 10.1016/j.immuni.2024.04.018. Epub 2024 May 13. PMID: 38744292.

Nicolle LE. Catheter associated urinary tract infections. Antimicrob Resist Infect Control. 2014 Jul 25;3:23. doi: 10.1186/2047-2994-3-23. PMID: 25075308; PMCID: PMC4114799.

Nielubowicz GR, Mobley HL. Host-pathogen interactions in urinary tract infection. Nat Rev Urol. 2010 Aug;7(8):430-41. doi: 10.1038/nrurol.2010.101. Epub 2010 Jul 20. PMID: 20647992.

Ogura T, Krosnowski K, Zhang L, Bekkerman M, Lin W. Chemoreception regulates chemical access to mouse vomeronasal organ: role of solitary chemosensory cells. PLoS One. 2010 Jul 30;5(7):e11924. doi: 10.1371/journal.pone.0011924. PMID: 20689832; PMCID: PMC2912856.

Ohmoto M, Matsumoto I, Yasuoka A, Yoshihara Y, Abe K. Genetic tracing of the gustatory and trigeminal neural pathways originating from T1R3-expressing taste receptor cells and solitary chemoreceptor cells. Mol Cell Neurosci. 2008 Aug;38(4):505-17. doi: 10.1016/j.mcn.2008.04.011. Epub 2008 May 2. PMID: 18539481.

Ohmoto M, Yamaguchi T, Yamashita J, Bachmanov AA, Hirota J, Matsumoto I. Pou2f3/Skn-1a is necessary for the generation or differentiation of solitary chemosensory cells in the anterior nasal cavity. Biosci Biotechnol Biochem. 2013;77(10):2154-6. doi: 10.1271/bbb.130454. Epub 2013 Oct 7. PMID: 24096675; PMCID: PMC3808513.

References

Ostrowski SM, Belkadi A, Loyd CM, Diaconu D, Ward NL. Cutaneous denervation of psoriasiform mouse skin improves acanthosis and inflammation in a sensory neuropeptide-dependent manner. J Invest Dermatol. 2011 Jul;131(7):1530-8. doi: 10.1038/jid.2011.60. Epub 2011 Apr 7. PMID: 21471984; PMCID: PMC3116081.

Pan J, Zhang L, Shao X, Huang J. Acetylcholine From Tuft Cells: The Updated Insights Beyond Its Immune and Chemosensory Functions. Front Cell Dev Biol. 2020 Jul 7;8:606. doi: 10.3389/fcell.2020.00606. PMID: 32733896; PMCID: PMC7359717.

Panneck AR, Rafiq A, Schütz B, Soultanova A, Deckmann K, Chubanov V, Gudermann T, Weihe E, Krasteva-Christ G, Grau V, del Rey A, Kummer W. Cholinergic epithelial cell with chemosensory traits in murine thymic medulla. Cell Tissue Res. 2014 Dec;358(3):737-48. doi: 10.1007/s00441-014-2002-x. Epub 2014 Oct 10. PMID: 25300645; PMCID: PMC4233111.

Pearson MM, Yep A, Smith SN, Mobley HL. Transcriptome of Proteus mirabilis in the murine urinary tract: virulence and nitrogen assimilation gene expression. Infect Immun. 2011 Jul;79(7):2619-31. doi: 10.1128/IAI.05152-11. Epub 2011 Apr 19. PMID: 21505083; PMCID: PMC3191972.

Perniss A, Boonen B, Tonack S, Thiel M, Poharkar K, Alnouri MW, Keshavarz M, Papadakis T, Wiegand S, Pfeil U, Richter K, Althaus M, Oberwinkler J, Schütz B, Boehm U, Offermanns S, Leinders-Zufall T, Zufall F, Kummer W. A succinate/SUCNR1-brush cell defense program in the tracheal epithelium. Sci Adv. 2023 Aug 2;9(31):eadg8842. doi: 10.1126/sciadv.adg8842. Epub 2023 Aug 2. PMID: 37531421 ; PMCID: PMC10396310.

Perniss A, Liu S, Boonen B, Keshavarz M, Ruppert AL, Timm T, Pfeil U, Soultanova A, Kusumakshi S, Delventhal L, Aydin Ö, Pyrski M, Deckmann K, Hain T, Schmidt N, Ewers C, Günther A, Lochnit G, Chubanov V, Gudermann T, Oberwinkler J, Klein J, Mikoshiba K, Leinders-Zufall T, Offermanns S, Schütz B, Boehm U, Zufall F, Bufe B, Kummer W. Chemosensory Cell-Derived Acetylcholine Drives Tracheal Mucociliary Clearance in Response to Virulence-Associated Formyl Peptides. Immunity. 2020 Apr 14;52(4):683-699.e11. doi: 10.1016/j.immuni.2020.03.005. PMID: 32294408.

Phillips JI, Davies I. The comparative morphology of the bladder and urethra in young and old female C57BL/Icrfat mice. Exp Gerontol. 1980;15(6):551-62. doi: 10.1016/0531-5565(80)90008-x. PMID: 7193592.

Pochini L, Scalise M, Galluccio M, Pani G, Siminovitch KA, Indiveri C. The human OCTN1 (SLC22A4) reconstituted in liposomes catalyzes acetylcholine transport which is defective in the mutant L503F associated to the Crohn's disease. Biochim Biophys Acta. 2012 Mar;1818(3):559-65. doi: 10.1016/j.bbamem.2011.12.014. Epub 2011 Dec 21. PMID: 22206629.

Pochini L, Tedesco GE, Mazza T, Scalise M, Indiveri C. OCTN1 mediates acetylcholine transport in the A549 lung cancer cells: possible pathophysiological implications. Front Mol Biosci. 2024 Dec 9;11:1512530. doi: 10.3389/fmolb.2024.1512530. PMID: 39719963; PMCID: PMC11666908.

Pomian A, Majkusiak W, Kociszewski J, Tomasik P, Horosz E, Zwierzchowska A, Lisik W, Barcz E. Demographic features of female urethra length. Neurourol Urodyn. 2018 Jun;37(5):1751-1756. doi: 10.1002/nau.23509. Epub 2018 Feb 10. PMID: 29427320.

Qiao Y, Sun Q, Chen X, He L, Wang D, Su R, Xue Y, Sun H, Wang H. Nuclear m6A reader YTHDC1 promotes muscle stem cell activation/proliferation by regulating mRNA splicing and nuclear export. Elife. 2023 Mar 9;12:e82703. doi: 10.7554/eLife.82703. PMID: 36892464; PMCID: PMC10089659.

References

Rane CK, Jackson SR, Pastore CF, Zhao G, Weiner AI, Patel NN, Herbert DR, Cohen NA, Vaughan AE. Development of solitary chemosensory cells in the distal lung after severe influenza injury. Am J Physiol Lung Cell Mol Physiol. 2019 Jun 1;316(6):L1141-L1149. doi: 10.1152/ajplung.00032.2019. Epub 2019 Mar 25. PMID: 30908939; PMCID: PMC6620670.

Rather LJ. Disturbance of function (functio laesa): the legendary fifth cardinal sign of inflammation, added by Galen to the four cardinal signs of Celsus. Bull N Y Acad Med. 1971 Mar;47(3):303-22. PMID: 5276838; PMCID: PMC1749862.

RHODIN J, DALHAMN T. Electron microscopy of the tracheal ciliated mucosa in rat. Z Zellforsch Mikrosk Anat. 1956;44(4):345-412. doi: 10.1007/BF00345847. PMID: 13353477.

Riera CE, Vogel H, Simon SA, Damak S, le Coutre J. Sensory attributes of complex tasting divalent salts are mediated by TRPM5 and TRPV1 channels. J Neurosci. 2009 Feb 25;29(8):2654-62. doi: 10.1523/JNEUROSCI.4694-08.2009. PMID: 19244541; PMCID: PMC6666243.

Rochlitzer S, Veres TZ, Kühne K, Prenzler F, Pilzner C, Knothe S, Winkler C, Lauenstein HD, Willart M, Hammad H, Müller M, Krug N, Lambrecht BN, Braun A. The neuropeptide calcitonin gene-related peptide affects allergic airway inflammation by modulating dendritic cell function. Clin Exp Allergy. 2011 Nov;41(11):1609-21. doi: 10.1111/j.1365-2222.2011.03822.x. Epub 2011 Jul 14. PMID: 21752117.

Roghani A, Feldman J, Kohan SA, Shirzadi A, Gundersen CB, Brecha N, Edwards RH. Molecular cloning of a putative vesicular transporter for acetylcholine. Proc Natl Acad Sci U S A. 1994 Oct 25;91(22):10620-4. doi: 10.1073/pnas.91.22.10620. PMID: 7938002; PMCID: PMC45073.

Ronald A. The etiology of urinary tract infection: traditional and emerging pathogens. Dis Mon. 2003 Feb;49(2):71-82. doi: 10.1067/mda.2003.8. PMID: 12601338.

Sann H, Pinter E, Szolcsányi J, Pierau FK. Peptidergic afferents might contribute to the regulation of skin blood flow. Agents Actions. 1988 Feb;23(1-2):14-5. doi: 10.1007/BF01967172. PMID: 3354377.

Saqui-Salces M, Keeley TM, Grosse AS, Qiao XT, El-Zaatari M, Gumucio DL, Samuelson LC, Merchant JL. Gastric tuft cells express DCLK1 and are expanded in hyperplasia. Histochem Cell Biol. 2011 Aug;136(2):191-204. doi: 10.1007/s00418-011-0831-1. Epub 2011 Jun 18. PMID: 21688022; PMCID: PMC3570962.

Saunders CJ, Christensen M, Finger TE, Tizzano M. Cholinergic neurotransmission links solitary chemosensory cells to nasal inflammation. Proc Natl Acad Sci U S A. 2014 Apr 22;111(16):6075-80. doi: 10.1073/pnas.1402251111. Epub 2014 Apr 7. PMID: 24711432; PMCID: PMC4000837.

Sawyer I, Smillie SJ, Bodkin JV, Fernandes E, O'Byrne KT, Brain SD. The vasoactive potential of kisspeptin-10 in the peripheral vasculature. PLoS One. 2011 Feb 9;6(2):e14671. doi: 10.1371/journal.pone.0014671. PMID: 21347414; PMCID: PMC3036649.

Sbarbati A, Crescimanno C, Benati D, Osculati F. Solitary chemosensory cells in the developing chemoreceptorial epithelium of the vallate papilla. J Neurocytol. 1998 Sep;27(9):631-5. doi: 10.1023/a:1006933528084. PMID: 10447237.

Schmidt P, Pfeil U, Lafee M, Petersen S, Perniss A, Keshavarz M, Das D, Wyatt A, Boehm U, Schütz B, Kummer W, Deckmann K. Tuft cells trigger neurogenic inflammation in the urethra. Cell Rep. 2025 Oct 28;44(10):116370. doi: 10.1016/j.celrep.2025.116370. Epub 2025 Sep 30. PMID: 41032411.

References

Schmiemann G, Kniehl E, Gebhardt K, Matejczyk MM, Hummers-Pradier E. The diagnosis of urinary tract infection: a systematic review. Dtsch Arztebl Int. 2010 May;107(21):361-7. doi: 10.3238/arztebl.2010.0361. Epub 2010 May 28. PMID: 20539810; PMCID: PMC2883276.

Schneider C. Tuft cell integration of luminal states and interaction modules in tissues. Pflugers Arch. 2021 Nov;473(11):1713-1722. doi: 10.1007/s00424-021-02630-2. Epub 2021 Oct 11. PMID: 34635955; PMCID: PMC8528756.

Schütz B, Jurastow I, Bader S, Ringer C, von Engelhardt J, Chubanov V, Gudermann T, Diener M, Kummer W, Krasteva-Christ G, Weihe E. Chemical coding and chemosensory properties of cholinergic brush cells in the mouse gastrointestinal and biliary tract. Front Physiol. 2015 Mar 24;6:87. doi: 10.3389/fphys.2015.00087. PMID: 25852573; PMCID: PMC4371653.

Shah AS, Ben-Shahar Y, Moninger TO, Kline JN, Welsh MJ. Motile cilia of human airway epithelia are chemosensory. Science. 2009 Aug 28;325(5944):1131-4. doi: 10.1126/science.1173869. Epub 2009 Jul 23. PMID: 19628819; PMCID: PMC2894709.

Shi Y, Massagué J. Mechanisms of TGF-beta signaling from cell membrane to the nucleus. Cell. 2003 Jun 13;113(6):685-700. doi: 10.1016/s0092-8674(03)00432-x. PMID: 12809600.

Shuman EK, Chenoweth CE. Recognition and prevention of healthcare-associated urinary tract infections in the intensive care unit. Crit Care Med. 2010 Aug;38(8 Suppl):S373-9. doi: 10.1097/CCM.0b013e3181e6ce8f. PMID: 20647795.

Song P, Rekow SS, Singleton CA, Sekhon HS, Dissen GA, Zhou M, Campling B, Lindstrom J, Spindel ER. Choline transporter-like protein 4 (CTL4) links to non-neuronal acetylcholine synthesis. J Neurochem. 2013 Aug;126(4):451-61. doi: 10.1111/jnc.12298. Epub 2013 Jun 25. PMID: 23651124; PMCID: PMC3866050.

Stamm WE, Norrby SR. Urinary tract infections: disease panorama and challenges. J Infect Dis. 2001 Mar 1;183 Suppl 1:S1-4. doi: 10.1086/318850. PMID: 11171002.

Steinhoff M, Ständer S, Seeliger S, Ansel JC, Schmelz M, Luger T. Modern aspects of cutaneous neurogenic inflammation. Arch Dermatol. 2003 Nov;139(11):1479-88. doi: 10.1001/archderm.139.11.1479. PMID: 14623709.

Strine MS, Wilen CB. Tuft cells are key mediators of interkingdom interactions at mucosal barrier surfaces. PLoS Pathog. 2022 Mar 10;18(3):e1010318. doi: 10.1371/journal.ppat.1010318. PMID: 35271673; PMCID: PMC8912186.

Tallini YN, Shui B, Greene KS, Deng KY, Doran R, Fisher PJ, Zipfel W, Kotlikoff MI. BAC transgenic mice express enhanced green fluorescent protein in central and peripheral cholinergic neurons. Physiol Genomics. 2006 Nov 27;27(3):391-7. doi: 10.1152/physiolgenomics.00092.2006. Epub 2006 Aug 29. PMID: 16940431.

Terlizzi ME, Gribaudo G, Maffei ME. UroPathogenic *Escherichia coli* (UPEC) Infections: Virulence Factors, Bladder Responses, Antibiotic, and Non-antibiotic Antimicrobial Strategies. Front Microbiol. 2017 Aug 15;8:1566. doi: 10.3389/fmicb.2017.01566. PMID: 28861072; PMCID: PMC5559502.

Tizzano M, Cristofoletti M, Sbarbati A, Finger TE. Expression of taste receptors in solitary chemosensory cells of rodent airways. BMC Pulm Med. 2011 Jan 13;11:3. doi: 10.1186/1471-2466-11-3. PMID: 21232137; PMCID: PMC3031280.

References

Tizzano M, Gulbransen BD, Vandenbeuch A, Clapp TR, Herman JP, Sibhatu HM, Churchill ME, Silver WL, Kinnamon SC, Finger TE. Nasal chemosensory cells use bitter taste signaling to detect irritants and bacterial signals. Proc Natl Acad Sci U S A. 2010 Feb 16;107(7):3210-5. doi: 10.1073/pnas.0911934107. Epub 2010 Jan 26. PMID: 20133764; PMCID: PMC2840287.

Tooyama I, Kimura H. A protein encoded by an alternative splice variant of choline acetyltransferase mRNA is localized preferentially in peripheral nerve cells and fibers. J Chem Neuroanat. 2000 Jan;17(4):217-26. doi: 10.1016/s0891-0618(99)00043-5. PMID: 10697248.

Treuting PM, Dintzis S, Montine KS (2017): Comparative Anatomy and Histology, A Mouse, Rat, and Human Atlas, Second Edition, Academic Press, London.

Urban DJ, Roth BL. DREADDs (designer receptors exclusively activated by designer drugs): chemogenetic tools with therapeutic utility. Annu Rev Pharmacol Toxicol. 2015;55:399-417. doi: 10.1146/annurev-pharmtox-010814-124803. Epub 2014 Sep 25. PMID: 25292433.

Vittoria A, La Mura E, Cocca T, Cecio A. Serotonin-, somatostatin- and chromogranin A-containing cells of the urethro-prostatic complex in the sheep. An immunocytochemical and immunofluorescent study. J Anat. 1990 Aug;171:169-78. PMID: 1981998; PMCID: PMC1257138.

Voisin T, Perner C, Messou MA, Shiers S, Ualiyeva S, Kanaoka Y, Price TJ, Sokol CL, Bankova LG, Austen KF, Chiu IM. The $CysLT_2R$ receptor mediates leukotriene C_4-driven acute and chronic itch. Proc Natl Acad Sci U S A. 2021 Mar 30;118(13):e2022087118. doi: 10.1073/pnas.2022087118. PMID: 33753496; PMCID: PMC8020753.

von Moltke J, Ji M, Liang HE, Locksley RM. Tuft-cell-derived IL-25 regulates an intestinal ILC2-epithelial response circuit. Nature. 2016 Jan 14;529(7585):221-5. doi: 10.1038/nature16161. Epub 2015 Dec 14. PMID: 26675736; PMCID: PMC4830391.

Wessler I, Kirkpatrick CJ, Racké K. Non-neuronal acetylcholine, a locally acting molecule, widely distributed in biological systems: expression and function in humans. Pharmacol Ther. 1998 Jan;77(1):59-79. doi: 10.1016/s0163-7258(97)00085-5. PMID: 9500159.

Wessler I, Roth E, Deutsch C, Brockerhoff P, Bittinger F, Kirkpatrick CJ, Kilbinger H. Release of non-neuronal acetylcholine from the isolated human placenta is mediated by organic cation transporters. Br J Pharmacol. 2001 Nov;134(5):951-6. doi: 10.1038/sj.bjp.0704335. PMID: 11682442; PMCID: PMC1573028.

Wiederhold S, Papadakis T, Chubanov V, Gudermann T, Krasteva-Christ G, Kummer W. A novel cholinergic epithelial cell with chemosensory traits in the murine conjunctiva. Int Immunopharmacol. 2015 Nov;29(1):45-50. doi: 10.1016/j.intimp.2015.06.027. Epub 2015 Jun 26. PMID: 26119492.

Williams TJ, Morley J. Prostaglandins as potentiators of increased vascular permeability in inflammation. Nature. 1973 Nov 23;246(5430):215-7. doi: 10.1038/246215a0. PMID: 4271544.

Winter DL. Receptor characteristics and conduction velocites in bladder afferents. J Psychiatr Res. 1971 Aug;8(3):225-35. doi: 10.1016/0022-3956(71)90021-5. PMID: 5112224.

Wolf-Johnston AS, Hanna-Mitchell AT, Buffington CA, Shinde S, Roppolo JR, Mayer E, Birder LA. Alterations in the non-neuronal acetylcholine synthesis and release machinery in esophageal epithelium. Life Sci. 2012 Nov 27;91(21-22):1065-9. doi: 10.1016/j.lfs.2012.04.028. Epub 2012 Apr 30. PMID: 22569297; PMCID: PMC3435437.

References

Yamashita J, Ohmoto M, Yamaguchi T, Matsumoto I, Hirota J. Skn-1a/Pou2f3 functions as a master regulator to generate Trpm5-expressing chemosensory cells in mice. PLoS One. 2017 Dec 7;12(12): e0189340. doi: 10.1371/journal.pone.0189340. PMID: 29216297; PMCID: PMC5720759.

Yasuhara O, Aimi Y, Shibano A, Kimura H. Primary sensory neurons containing choline acetyltransferase of the peripheral type in the rat trigeminal ganglion and their relation to neuropeptides-, calbindin- and nitric oxide synthase-containing cells. Brain Res. 2007 Apr 13;1141:92-8. doi: 10.1016/j.brainres.2007.01.025. Epub 2007 Jan 12. PMID: 17291466.

Yoshimura N, Seki S, Erickson KA, Erickson VL, Hancellor MB, de Groat WC. Histological and electrical properties of rat dorsal root ganglion neurons innervating the lower urinary tract. J Neurosci. 2003 May 15;23(10):4355-61. doi: 10.1523/JNEUROSCI.23-10-04355.2003. PMID: 12764124; PMCID: PMC6741085.

Zarb P, Coignard B, Griskeviciene J, Muller A, Vankerckhoven V, Weist K, Goossens M, Vaerenberg S, Hopkins S, Catry B, Monnet D, Goossens H, Suetens C; National Contact Points for the ECDC pilot point prevalence survey; Hospital Contact Points for the ECDC pilot point prevalence survey. The European Centre for Disease Prevention and Control (ECDC) pilot point prevalence survey of healthcare-associated infections and antimicrobial use. Euro Surveill. 2012 Nov 15;17(46):20316. doi: 10.2807/ese.17.46.20316-en. PMID: 23171822.

Zhang Y, Hoon MA, Chandrashekar J, Mueller KL, Cook B, Wu D, Zuker CS, Ryba NJ. Coding of sweet, bitter, and umami tastes: different receptor cells sharing similar signaling pathways. Cell. 2003 Feb 7;112(3):293-301. doi: 10.1016/s0092-8674(03)00071-0. PMID: 12581520.

Zhao S, Ting JT, Atallah HE, Qiu L, Tan J, Gloss B, Augustine GJ, Deisseroth K, Luo M, Graybiel AM, Feng G. Cell type–specific channelrhodopsin-2 transgenic mice for optogenetic dissection of neural circuitry function. Nat Methods. 2011 Sep;8(9):745-52. doi: 10.1038/nmeth.1668. PMID: 21985008; PMCID: PMC3191888.

Zheng X, Tizzano M, Redding K, He J, Peng X, Jiang P, Xu X, Zhou X, Margolskee RF. Gingival solitary chemosensory cells are immune sentinels for periodontitis. Nat Commun. 2019 Oct 3;10(1):4496. doi: 10.1038/s41467-019-12505-x. PMID: 31582750; PMCID: PMC6776549.

Ehrenwörtliche Erklärung

Ehrenwörtliche Erklärung

„Hiermit erkläre ich, dass ich die vorliegende Arbeit selbständig und ohne unzulässige Hilfe oder Benutzung anderer als der angegebenen Hilfsmittel angefertigt habe. Alle Textstellen, die wörtlich oder sinngemäß aus veröffentlichten oder nichtveröffentlichten Schriften entnommen sind, und alle Angaben, die auf mündlichen Auskünften beruhen, sind als solche kenntlich gemacht. Bei den von mir durchgeführten und in der Dissertation erwähnten Untersuchungen habe ich die Grundsätze guter wissenschaftlicher Praxis, wie sie in der „Satzung der Justus-Liebig-Universität Gießen zur Sicherung guter wissenschaftlicher Praxis" niedergelegt sind, eingehalten sowie ethische, datenschutzrechtliche und tierschutzrechtliche Grundsätze befolgt. Ich versichere, dass Dritte von mir weder unmittelbar noch mittelbar geldwerte Leistungen für Arbeiten erhalten haben, die im Zusammenhang mit dem Inhalt der vorgelegten Dissertation stehen. Die vorgelegte Arbeit wurde weder im Inland noch im Ausland in gleicher oder ähnlicher Form einer anderen Prüfungsbehörde zum Zweck einer Promotion oder eines anderen Prüfungsverfahrens vorgelegt. Alles aus anderen Quellen und von anderen Personen übernommene Material, das in der Arbeit verwendet wurde oder auf welches direkt Bezug genommen wird, wurde als solches kenntlich gemacht. Insbesondere wurden alle Personen genannt, die direkt und indirekt an der Entstehung der vorliegenden Arbeit beteiligt waren. Mit der Überprüfung meiner Arbeit durch eine Plagiatserkennungssoftware bzw. ein internetbasiertes Softwareprogramm erkläre ich mich einverstanden."

Acknowledgment

I gratefully acknowledge the generous financial support provided by *Al-Ahliyya Amman University* (AAU) and Justus Liebig University Giessen.

My deepest appreciation goes to my supervisor, **Professor Wolfgang Kummer**, whose guidance, encouragement, and insightful advice made this work possible. His support accompanied me throughout every stage of this project.

I extend my sincere thanks to my colleagues and the entire research group. I am especially grateful to **Dr. Klaus Deckmann**, **Dr. Burkhard Schütz, Dr. Uwe Pfeil, Mr. Adriano Sanna, Mrs. Aysegül Demiral, Mrs. Petra Mermer, Mrs. Tamara Papadakis, Mrs. Silke Wiegandand Mr. Martin Bodenbenner-Türich** for their exceptional cooperation and assistance. And special thanks to Prof. Dr. Ulrich Boehm team: Department of Pharmacology and Toxicology, University of Saarland School of Medicine especially Mrs. Amanda Wyatt and Mr. Das Debajyoti.

My heartfelt thanks go to **Ms. Patricia Berger** for her remarkable support and guidance from the very beginning of my studies to their completion.

Very special thanks are due to my wife, **Dima Hamarsheh**, for her unwavering support, patience, and encouragement at every step of this journey. Her presence helped me stay grounded during the most challenging moments of my thesis.

I am also profoundly grateful to my family—my father **Khaleel (May his soul rest in peace)**, my mother **Sameeha**, my daughters **Rahaf and Rose**, my brothers **Muhannad, Izzat and Mohammad**, my sisters **May**, **Maha** and **Watan** and my wife's family—for their continuous love, support, and understanding throughout these years.

Finally, I thank God for guiding me through every difficulty. Your presence has sustained me day by day, and I remain grateful for the strength that allowed me to complete this degree. I will continue to trust in Your guidance for the future.